CHAPTER 8

Ionic Polymerisation and New Approaches to Polymerisation under Flow Conditions

LAURENS BROCKEN AND IAN R. BAXENDALE*

Department of Chemistry, University of Durham, South Road, Durham DH1 3LE, UK
*Email: i.r.baxendale@durham.ac.uk

8.1 Ionic Polymerisation

In ionic polymerisation chain-growth proceeds through an active charged end group, involving either a negative charge, anionic polymerisation, or a positive charge, cationic polymerisation. Inevitably anionic polymerisation is limited to monomers possessing an electron-withdrawing group, whereas cationic polymerisation necessitates the monomers to have electron-donating substituents. The advantage of ionic polymerisation over radical polymerisation is the higher control over the parameters of dispersity and molecular weight. The main drawback of ionic polymerisation is its high sensitivity to impurities in the solvents and starting materials and high variation response to even small changes in processing parameters. Indeed, the concentration of the different charged species and the degree of the ion pairing will affect intrinsic stability and reactivity of the polymerising intermediates, which are impacted upon by the reaction conditions but principally by the polarity of the reaction medium. In general loose ion pairs will be much more reactive than contact ion pairs. However, the further

Green Chemistry Series No. 62
Flow Chemistry: Integrated Approaches for Practical Applications
Edited by Santiago V. Luis and Eduardo Garcia-Verdugo

Published by the Royal Society of Chemistry, www.rsc.org

coordination environment and solvation of the various ions can drastically attenuate their propagating potential.

Living anionic polymerisation was first comprehensively performed in flow as a means to study polymerisation kinetics. This research was undertaken by Szwarc *et al.* and Schulz *et al.* in the mid-sixties.[1–6] The technique then lay dormant for a time before being expanded upon recently by Müller *et al.* who investigated the living anionic polymerisation of 2-vinylpyridine and styrene in continuous flow.[7]

Two different flow set-ups were compared. The first used an interdigital micromixer, resulting in laminar mixing. The second set-up used a tangential four-way jet mixing device resulting in a more turbulent flow regime (Figure 8.1). It quickly became clear that the turbulent four-way jet mixing device produced more defined dispersity and highlighted the importance of mixing. Normally anionic polymerisations in batch need to be performed at low temperatures (*e.g.* −78 °C) to allow control. Beneficially due to the high surface to volume ratio in the flow reactor, these reactions could instead be performed at room temperature.

Traditionally a key aspect of controlled living cationic polymerisations is limiting the concentration of the active propagating species; this is highlighted by the Winstein equilibrium[8] (Figure 8.2). Reducing the proportion of active species instils a degree of control over the polymerisation process especially when the exchange between the different active/dormant species is faster than any propagation step. Under these conditions control of M_n is possible as well as a reduction in negative events such as

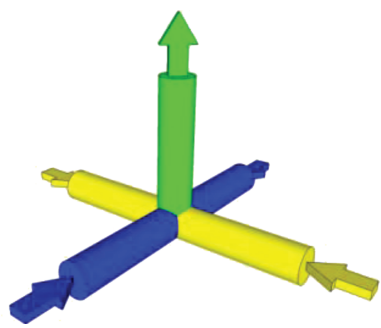

Figure 8.1 Operating principal of the four-way jet mixing device; blue stream 1 and yellow stream 2 combine to create a single flow stream green.

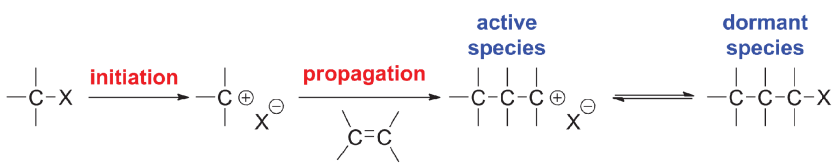

Figure 8.2 Winstein equilibrium.

chain-breaking processes, termination and transfer reactions. The downside of such a scenario is a slow polymerisation process due to the low concentration of active species. To challenge this paradigm Nagaki *et al.*[9] elected to investigate the impact of combining a highly reactive initiator with very fast and efficient mixing provided by a microfluidics device to investigate if control could be achieved over molecular weight and dispersity even in reactions where the equilibrium did not favour the dormant species.

An *N*-acyliminium ion was generated by low-temperature electrochemical oxidation in batch and combined with the monomer *via* a micromixer system and passed into a microtube residence time reactor before a quench solution of $i\text{Pr}_2\text{NH}/\text{CH}_2\text{Cl}_2$ was introduced to stop the polymerisation (Figure 8.3). It was found that the polymerisation was complete within a short residence time of 0.5 s. The M_n increased linearly with an increase in the quantity of monomer used indicating the lack of transfer competing reactions and excellent control over dispersity was achieved (Table 8.1).

Tani *et al.* utilized the same general reactor configuration to perform cationic polymerisation of isopropyl vinyl ether using a brominated dendritic initiator to prepare branch hybrid polymers (Figure 8.4).[10] The

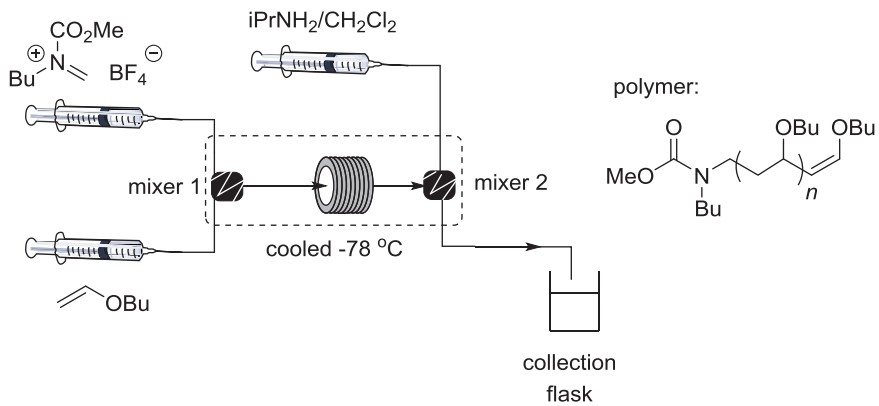

Figure 8.3 Microsystem for polymerisation. Mixer 1: A 40 μm channel multilamination-type micromixer manufactured by Institut für Mikrotechnik Mainz GmbH. Mixer 2: A splitting and recombination-type micromixer manufactured by Yamatake as YM-1.

Table 8.1 Cationic polymerisation of vinyl ether initiated by *N*-acyliminium.

Monomer (equiv)	M_n^{app} (g mol^{-1})	$Đ$
10	15 000	1.40
25	29 000	1.26
32	44 000	1.17
50	67 000	1.14

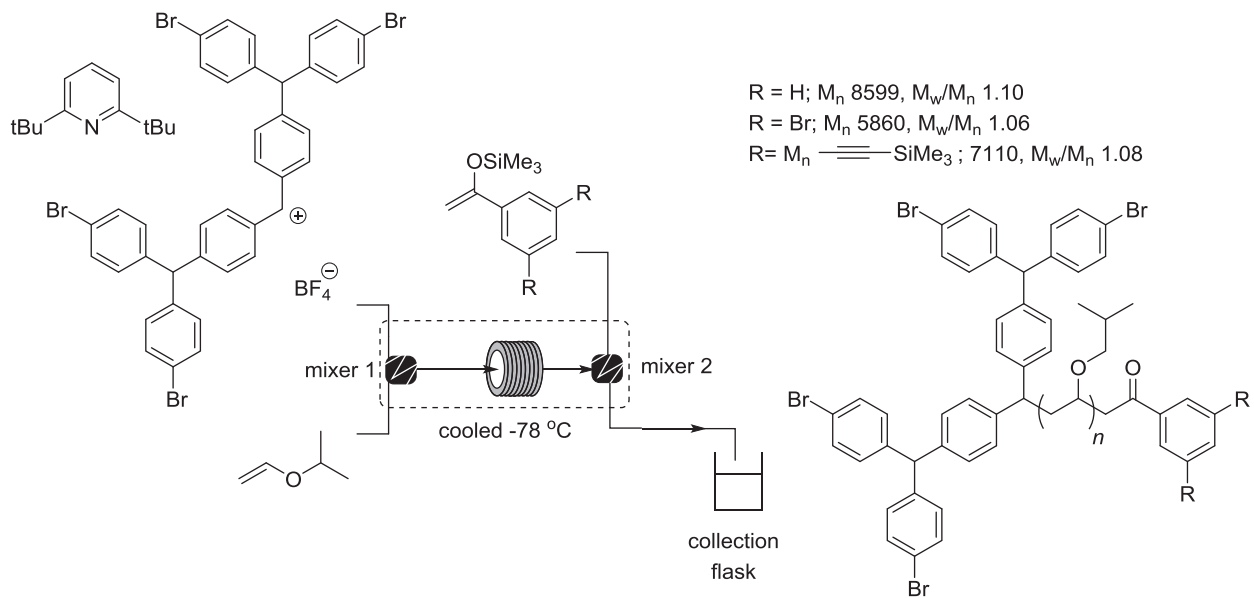

Figure 8.4 Linear-dendritic hybrid polymers prepared in flow.

incorporated aryl bromides were subsequently further functionalised using Suzuki–Miyaura coupling and a copper catalysed azide/alkyne click cycloaddition was applied to the acetylene expanding the range of available end groups. Again, the cationic initiator was first synthesised by electrochemical anodic oxidation and then introduced to the flow reactor where the polymerisation and quenching steps were conducted. Interestingly, the terminator unit used was a silyl enol ether which allowed additional functionality to be easily introduced in the form of aromatic ketones. Analysis by size exclusion chromatography indicated a narrow weight distribution profile for all the polymers synthesised.

Lu *et al.* has used aluminium trichloride promoted initiation of isobutylene.[11,12] For this very reactive monomer they highlighted the enhanced quality of the polymer that could be gained through the improved mixing and residence time control in flow. Under optimised conditions M_n ranges from 20–100 $kg\,mol^{-1}$ could be reproducibly accessed in ~6 s at relatively high temperatures for this type of polymerisation (up to −10 °C, normally −60 °C is required in batch). The key to the high performance of the reactor was the use of in-line heat exchangers and micromixers. This highlights again the value of flow chemistry to very fast and exothermic chemistries. Indeed, Ulitin and Tereshchenko have created a mathematical simulation of the macrokinetics for the catalysed process allowing predictions to be made regarding the best reactor geometries and flow velocities to prepare different compositions of butyl rubber.[13]

Rapid mixing or flash chemistry has been applied to the related butyl lithium initiated anionic polymerisation of styrene in flow.[14] In addition the polymer's living end could be trapped by with 1,1-diphenylethylene and this organometallic used as a macro initiator for further anionic polymerisation of acrylates to form diblock copolymers (Figure 8.5). Only very short residence times (2.92–4.38 s) were required for each step. As an illustration a series of styrene/MMA co-polymers were generated with an M_n range of 3.9–9 $kg\,mol^{-1}$ and dispersity of 1.14–1.30.

It was further shown that substituted styrenes, such as *p*-dimethylsilylstyrene could be used along with different alkyl methacrylates (*t*BuMA, and *n*BuMA) including by sequentially adding different acrylates to produce triblock polymers.

More recently, Nyrop *et al.* published an article comparing flow and batch polymerisation for the synthesis of vinyl ether terpolymers.[15] Their report focused on the preparation of polymer – iRNA (small interfering ribonucleic acid, siRNA is double stranded RNA and has a typical length of 20–25 base pairs) conjugates for utilisation in biomedical and medicinal chemistry. Specifically for such medicinal applications the ability to accurately control the polymeric structure was critical. A cationic polymerisation was chosen to generate vinyl ether terpolymers using $BF_3{\cdot}OEt_2$ as a Lewis acid catalyst. The polymers derived from flow processing were shown to be reproducibly more consistent and therefore better starting materials for formulation of the

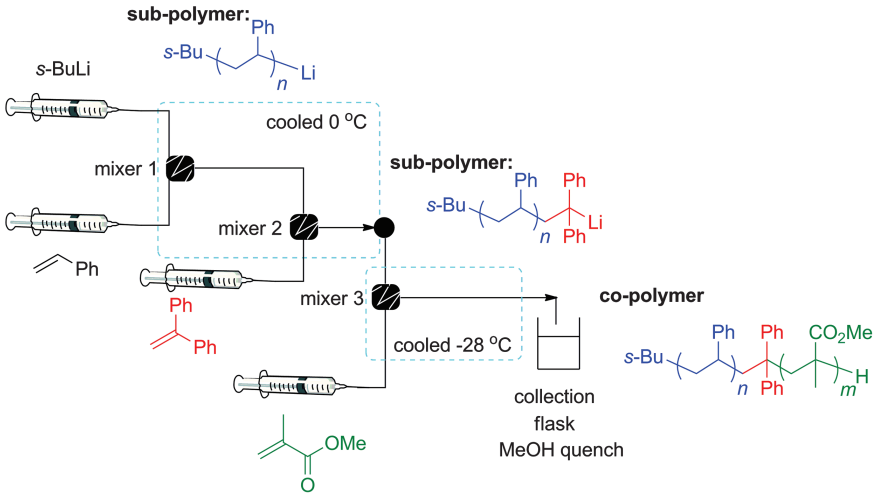

Figure 8.5 Flow-microreactor-system-controlled block copolymerisation of styrene and methyl methacrylate (MMA).

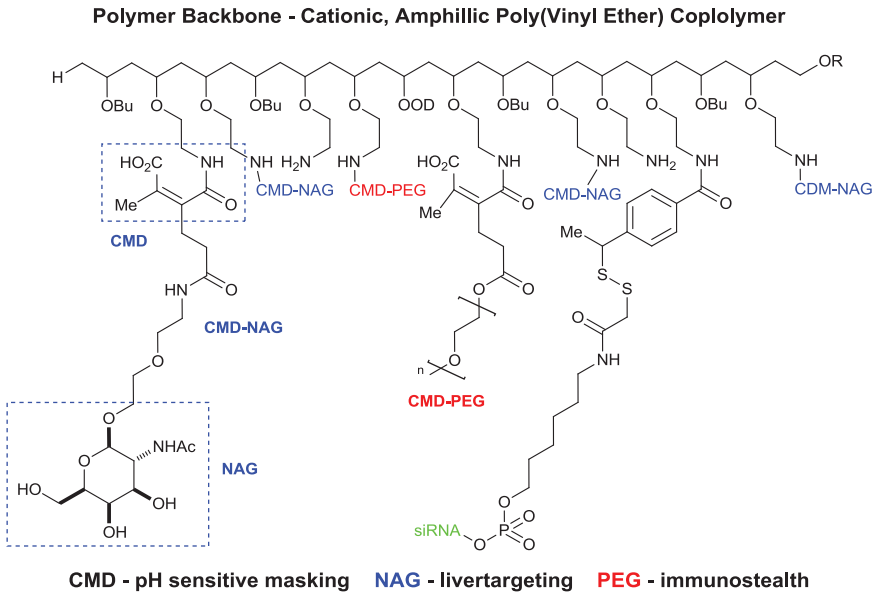

Figure 8.6 Polymer–siRNA conjugate.

polymer–siRNA conjugates. This was highlighted through the better *in vivo* performance of the generated conjugates (Figure 8.6).

The relief of bond-angle ring strain or reduction of steric repulsion in certain cyclic precursor favours ring opening polymerisation (ROP).[16] Several groups have investigated the use of flow reactors as tools to help with issues

of enhanced thermal dissipation or better mixing to instil greater reaction control. In an early example Wilms *et al.*[17] realised the preparation of hyperbranched polyglycerol in a flow reactor through the highly strained epoxide ring-opening polymerisation of glycidol. A stainless steel slit-interdigital micromixer (Figure 7.10; Chapter 7) was used to blend the pre-heated solutions of trimethylol propane (TMP) and glycidol before passage into a residence time coil of 10 mL internal volume (Figure 8.7).

In order to avoid compounding issues associated increased viscosity impacting mixing or leading to blockage a target $M_n = 1000\ g\,mol^{-1}$ was initially selected. A molar ratio Initiator/Monomer of 1 : 11.7 gave a polymer of $M_n = 1100\ g\,mol^{-1}$ with an average degree of polymerisation of 13 and (15 hydroxyl end groups) in ~5.5 min total residence time. Further conditions were tested changing flow rates and relative ratios of initiator and monomer resulting in higher molecular weight species being produced; overall the system performed well and was highlighted as an excellent replacement for traditional batch synthesis of such polymers.

The cationic ring-opening polymerisation of 2-ethyl-2-oxazoline under flow conditions has been performed. The general polymerisation mechanism is shown in Figure 8.8. The synthesis of such polymers have historically mainly been conducted at a laboratory scale as polymerisation times in batch are extended requiring in excess of 10 h and there are several reported problems regarding scale up, like strong reaction exotherms.[18–20] It has been shown that a reduction in the reaction time could be obtained *via* microwave assisted polymerisation (<1 min, 200 °C; although side reactions occurred above 140 °C)[20–22] which inspired Paulus *et al.*[23] to investigate applying microwave irradiation to a flow reactor. A CEM Voyager™ mono-modal microwave system (max 300 W temperature regulated power) was used investigating a selection of glass (straight tube and coil) and Teflon coil inserts as well as running a scaled CSTR microwave reactor. The glass coil performed best which when run a set temperature of 140 °C enabled full conversion of 2-ethyl-2-oxazoline at a throughput of 0.144 mol h^{-1} (~16.7 min theoretical residence time) delivering a polymer of M_n 13.5 kg mol^{-1} and dispersity of 1.42 (analysed by GPC).

Building on the flow results of Paulus *et al.* and noting evidence that a pressurised batch reactor[24] had also been very effective Baeten *et al.*[25] investigated a flow chemistry approach to extend the reactivity patterns leading to mono-, di- and tri-block (co-)polymers.

The polymerisation of 2-ethyl-2-oxazoline (EtOx) and *n*-propyl-2-oxazoline (*n*PropOx) showed a high temperature dependence on conversion and to a certain extent on the average number molecular weight. The dispersity remained essentially constant for the various temperatures for both monomers (Tables 8.2 and 8.3). Furthermore, no significant side reactions were observed. These results showed that flow chemistry is a valuable technique and thus opened the way to prepare di-block polymerisation and tri-block polymerisation which gave similar results compared to the mono-polymerisation (Table 8.4).

The continuous flow ring-opening polymerisation of various lactone or lactide derived monomers is an important research area for the preparation

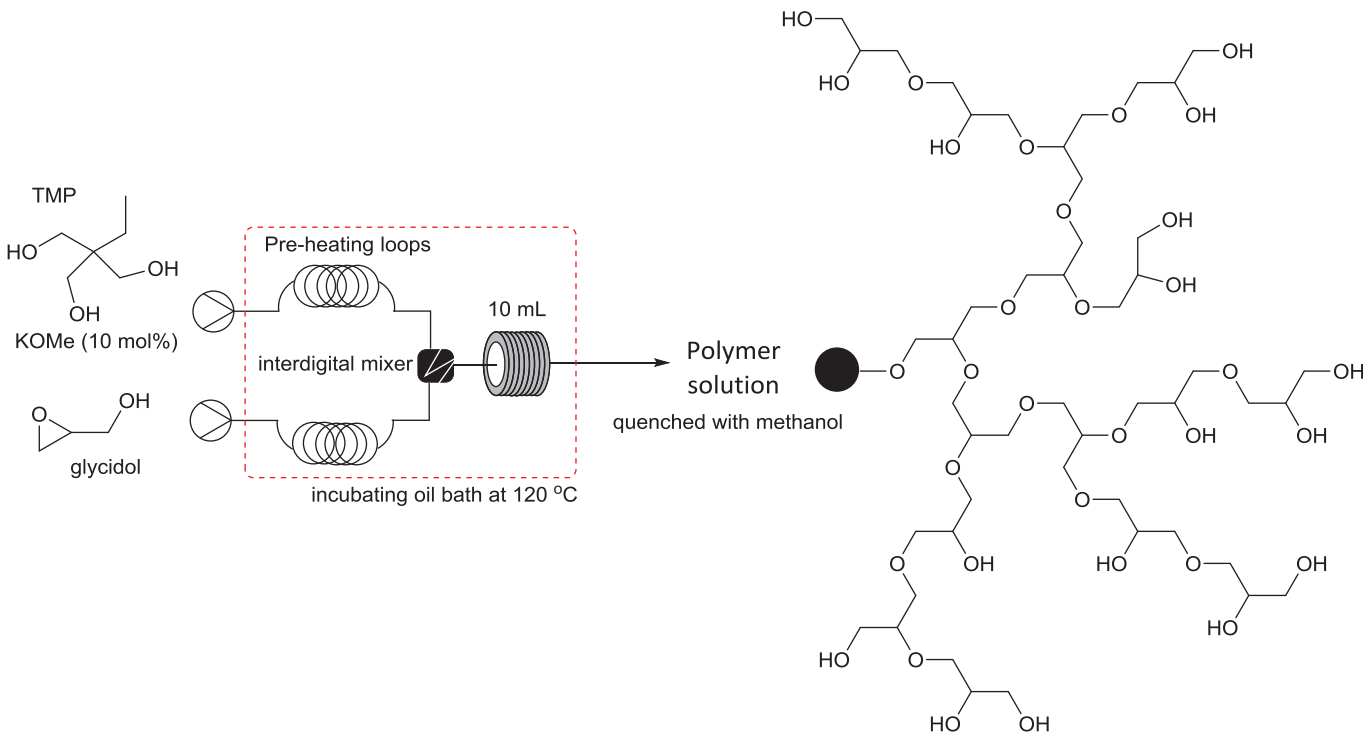

Figure 8.7 Ring-opening polymerisation of glycidol in flow.

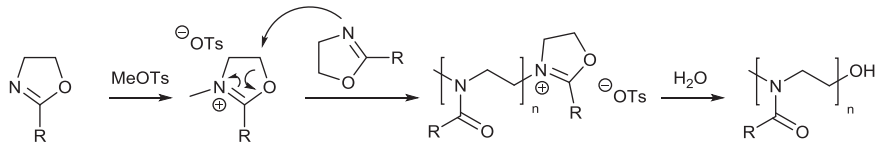

Figure 8.8 General cationic ring-opening polymerisations of 2-oxazolines.

Table 8.2 2-Ethyl-2-oxazoline (EtOx) homo-polymerisation achieving full monomer conversion.

Temperature (°C)	Residence time (min)	Conversion (%)	M_n^{app} (g mol^{-1})	$Đ$
140	12.5	100	9760	1.15
160	5	100	10 240	1.11
180	2	100	10 280	1.12

Table 8.3 *n*-Propyl-2-oxazoline (*n*PropOx) homo-polymerisation achieving full monomer conversion.

Temperature (°C)	Residence time (min)	Conversion (%)	M_n^{app} (g mol^{-1})	$Đ$
140	12.5	99.3	8950	1.24
160	5	100	8170	1.23
180	2	99.5	9240	1.16

Table 8.4 Block co-polymerisation of 2-ethyl-2-oxazoline (EtOx) and *n*-propyl-2-oxazoline (*n*PropOx) at 160 °C and 5 min residence time.[a]

Polymer	M_n^{app} (g mol^{-1})	$Đ$	M_p^{app} (g mol^{-1})	Ratio
EtOx	3510	1.10	3740	—
EtOx-*b*-*n*PropOx	6140	1.12	7130	1/1.18
EtOx-*b*-*n*PropOx-*b*-EtOx	7400	1.25	10 910	2/1.02
*n*PropOx	3940	1.09	4210	—
*n*PropOx-*b*-EtOx	5540	1.17	6490	1/0.85
*n*PropOx-*b*-EtOx-*b*-*n*PropOx	7320	1.21	9660	2/1.11

[a] M_n^{app} apparent molecular weight. M_p^{app} apparent proposed molecular weight.

of biodegradable and biocompatible materials.[26–32] With ever increasing environmental concerns driving the demand for degradable aliphatic polymers, such systems are becoming increasingly popular. One simple strategy employed under flow conditions has been the reinvestigation of the classical tin triflate catalysed ROP of ε-caprolactone.[33] A simple PTFE tubular reactor was constructed and used for the ROP at 80 and 110 °C in the presence of benzyl alcohol as the initiator (Figure 8.9). It was reported that improved control over the processing conditions compared to batch gave a higher fidelity of the polymer product being produced in terms of M_n and dispersity.

In a follow-up paper Zhu *et al.* used a modified approach involving initiation with 6-mercapto-1-hexanol thiol (substituted for the benzyl alcohol)

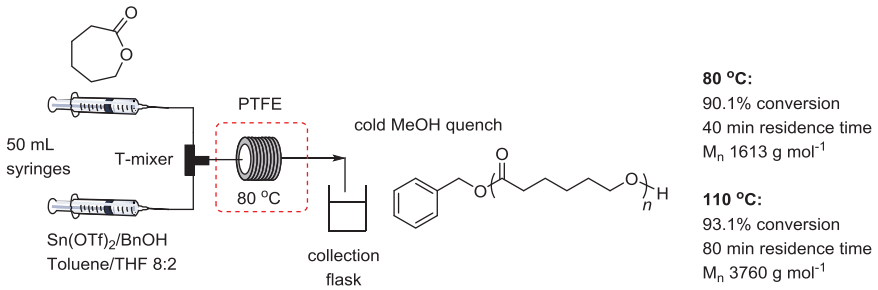

Figure 8.9 Microreactor system for $Sn(OTf)_2$ catalysed ROP.

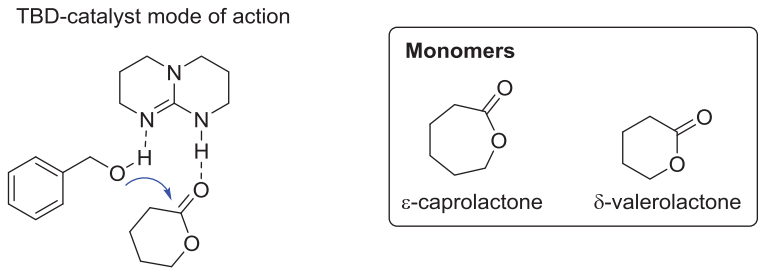

Figure 8.10 1,5,7-triazabicyclodecene bifunctional organocatalysis of the ROP.

in the presence of the tin triflate catalyst to furnish thiol terminated poly(ε-caprolactone) (PLC).[34] A lower reactor temperature of 50 °C was used (99% conversion) with a longer residence time of 120 min to generate a polymer with M_n 1470 g mol^{-1} and narrow dispersity of 1.12. A kinetic comparison between the flow polymerisation and an equivalent batch process showed an increased reactivity of the flow system of between 4–7 times this was ascribed to the improved mixing and heat transfer.

Another approach investigated by Zhu *et al.* was the use of hydride Brønsted acid/H-binding bifunctional organocatalysis of the ROP.[35] The organic base 1,5,7-triazabicyclodecene (TBD) was selected and assessed in flow for the processing of two monomers ε-caprolactone and δ-valerolactone using again the simple PTFE assembled flow system (Figures 8.9 and 8.10). Interestingly, the homopolymerisations of both monomers in flow gave products of higher molecular weight than those prepared analogously in batch which was resultant of a generally higher monomer conversion under the flow conditions (Table 8.5). The reactions were run at room temperature and with very low levels of the TBD catalyst 0.5 mol%.

The investigation was also extended to examine block co-polymerisations of the lactones *via* sequential introduction of the monomers as part of an integrated flow reaction in an extended reactor configuration (Figure 8.11).

An equivalent organocatalytic approach has also been used for the polymerisation of L-lactide with bifunctional initiators (bicyclononyne and

Table 8.5 Ring opening polymerisation of ε-caprolactone and δ-valerolactone comparative batch and flow results.[a]

Monomer	Method	Conversion (%)	Reaction time (min)	M_n (g mol^{-1})	$Đ$
ε-caprolactone	Batch	10.1	30	1320	1.05
ε-caprolactone	Flow	18.1	30	2290	1.05
ε-caprolactone	Batch	14.9	60	1870	1.06
ε-caprolactone	Flow	29.5	60	3480	1.04
δ-valerolactone	Batch	35.7	6	2220	1.08
δ-valerolactone	Flow	66.3	6	6830	1.07
δ-valerolactone	Batch	71.6	15	7450	1.09
δ-valerolactone	Flow	90.0	15	9120	1.08

[a] M_n molecular weight – determined by ^{1}H NMR. $Đ$ determined by SEC.

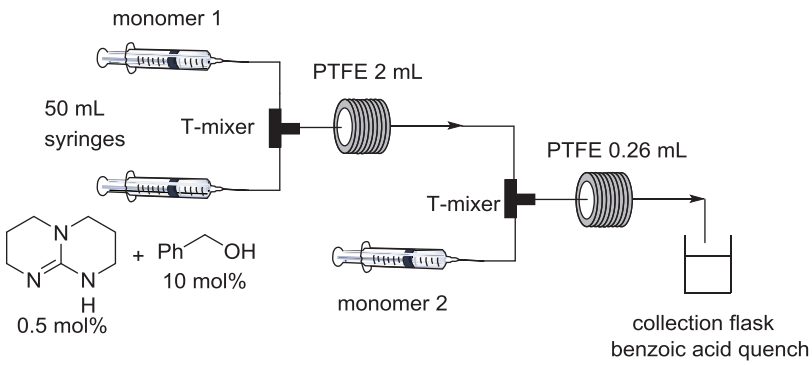

Polymer	Rt 1	DP 1	dispersity 1	Rt 2	DP	dispersity 2
PVL-*b*-PCL	10	11	1.07	90	21	1.09
PCL-*b*-PVL	90	11	1.05	10	21	1.08

Rt = Residence time

DP = Degree polymerisation

Figure 8.11 Ring opening co-polymerisation in flow.

tetrazine containing) meaning after polymerisation the material could be further conjugated using click type chemistries on the end capping groups to generate products for biomedical applications.[36] A small 1 μL mixing chip was initially used to investigate the polymerisation (Figure 8.12). The ratio between the monomer and initiator was maintained (80 : 1) whilst catalyst loading (0.1–1.2 mol%), temperature (−10 to 30 °C) and residence times (2–5 s) were varied. However, ultimately it was shown that much longer residence time of (up to 30 s) were required for effective polymerisation and so the microchip was replaced with a coil reactor. This allowed an optimised 98% conversion in a 20 s residence time, 0.6 mol% catalyst at 30 °C.

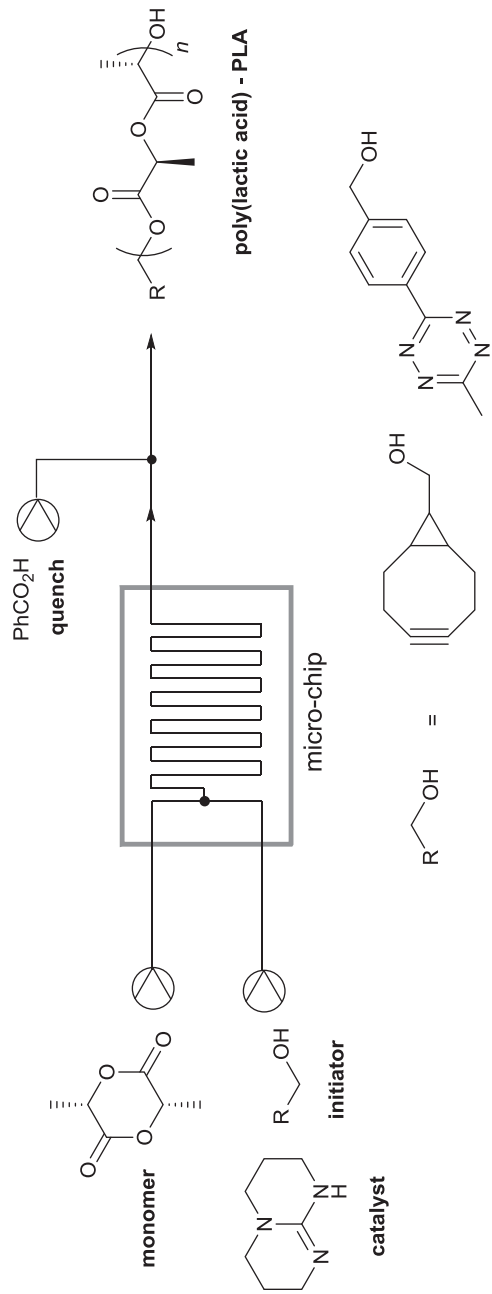

Figure 8.12 Synthesis of poly(lactic acid) *via* ring opening co-polymerisation in flow.

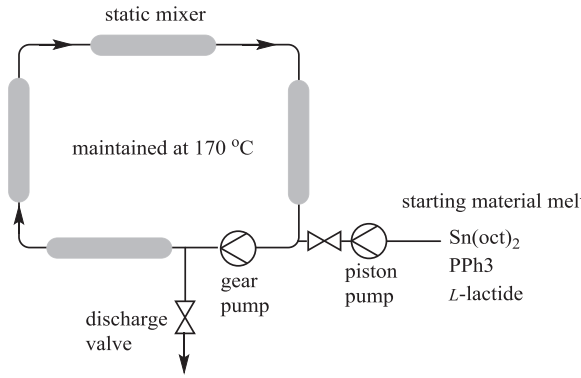

Figure 8.13 Schematic of the tubular static mixing reactor (TSMR) used for synthesis of poly(lactic acid).

In general conversion was shown to increase as the reaction temperature was reduced which is consistent with the exothermic transformation of monomer to polymer due to the enthalpic contribution provided by the release of ring strain. At low catalyst loading the process is, therefore, operating under kinetic control due to the short residence times and rapid quenching.

A larger scale hot melt synthesis of poly(lactic acid) has been performed using a reactor loop with embedded static mixing elements – a tubular static mixing reactor (TSMR) (Figure 8.13).[37] Each static mixer was 500 mm long comprising of 19 individual element made from 6 corrugated plates forming channels at 45° to the main axis of the tubular pipe with adjacent elements positioned perpendicular to enhance mixing. Circulation of the blend was performed for 90 min before the material was discharged and rapidly cooled, the resultant polymer had a molecular weight of 166 kg mol^{-1} and dispersity $Đ = 1.48$. Although not truly representing a continuous production solution this work is a good starting point for the future industrial production of poly(lactic acid) *via* a flow process.

The anionic polymerisation of cyclic phosphates has been investigated by Baeten *et al.*[38] using a flow chip-based reactor, again organocatalysis was used to promote the reaction. A combination of 1,8-diazobicyclo[5.4.0]undec-7-ene (DBU) as the base in the presence of a thiourea (TU) or TBD as a bifunctional catalyst was first studied for the polymerisation of 2-isobutoxy-2-oxo-1,3,2-dioxaphospholone (Figure 8.14; R = *i*Bu). At 0 °C 93% conversion was obtained in a residence time of 20 min, the molecular weight distribution was determined by SEC <1.15 for a molecular weight of 2440 g mol^{-1}. The reaction was accelerated by heating at 40 °C leading to an equitable polymer in 7.5 min (94% conversion, M_n 2348 g mol^{-1}, $Đ = 1.18$).

Next, a second polymerisation of 2-butenoxy-2-oxo-1,3,2-dioxaphospholane (Figure 8.14; R–$CH_2CH_2CH{=}CH_2$) was run achieving similar results (10 min, 40 °C, 94% conversion, M_n 2800 g mol^{-1}, $Đ = 1.20$). It was also shown that the system could be run uninterrupted for 7.5 h

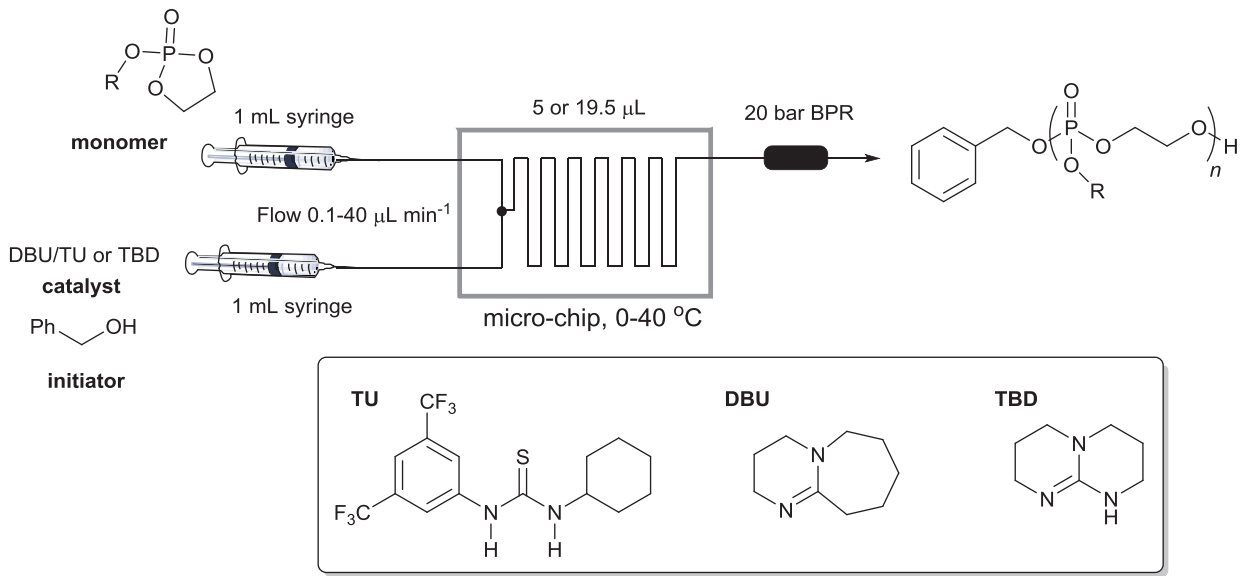

Figure 8.14 Organocatalysed anionic ring-opening polymerisation of a cyclic phosphate in flow.

allowing easy scale up. In an interesting variation the authors investigated the post-functionalisation of the pendant alkene unit (Figure 8.14; R–$CH_2CH_2CH{=}CH_2$) using a UV-induced radical thiol–ene reaction as a conjugation process. Indeed, by simply appending a UV-irradiated second flow microchip to the end of the polymerisation process the coupling reaction could be integrated to create a multi-step sequence (Figure 8.15). This resulted in a residence time of 10 min for the polymerisation and 65 s for the subsequent UV process, a final polymer conjugate was obtained which gave analysis of M_n 6220 g mol^{-1}, $Đ = 1.34$.

8.2 Photo-polymerisation

Over the last decade photochemistry has become increasingly popular with its adoption as a 'green' chemistry approach. This popularisation of the activation of reactions with photons has also been seen through the adoption of more photo-polymerisation.[39] The advantage of adopting a flow set-up to conduct this type of chemistry results from the small reactor geometries. In a batch reactor a light gradient will occur due to the absorption of light by the preceding outer volume (Beer–Lambert law). Consequently, scaling up the reaction may prove difficult and produce unpredictable results as reaction kinetics vary widely due to the type, shape and size of reaction vessel chosen. It has been shown that many different reactions can be performed more consistently using photo-flow reactors.[40,41] In many cases resulting in improved yields/conversions and a reduction in processing times in certain cases from days to minutes.

Eckardt *et al.*[42] have described the synthesis of branched poly(butyl acrylate)s with tri(propylene glycol) diacrylate (TPGDA) crosslinkers using photo-induced free radical polymerisation. Often using this technique gelation occurs, however, it has been shown that the addition of a chain transfer agent, mainly an alkane thiol, can suppress this issue, this approach has become termed the 'Strathclyde method'.[43] To facilitate continuous synthesis a simple tubular photoflow reactor was assembled by tightly wrapping PFA tubing (ID 0.75 mm) around the casing of a 15 W UV-light tube ($\lambda_{max} = 365$ nm) (Figure 8.16). An HPLC pump was used to deliver the reactant stream. To highlight any differences between the photo-flow and batch polymerisations several polymers with varying molar masses were synthesized (Table 8.6).

A general trend for higher conversion with an associated increase in M_n and M_w (broader molecular weight distribution) was observed in flow. It was noted the temperature of the photo-flow reactor was regulated at >65 °C due to improved heat transfer, whereas the photo-batch reactor recorded temperatures >90 °C. The scalability and robustness of the system was shown by performing a continuous providing over 300 g of branched polymer during a 24 h run.

The UV photopolymerisation of *n*-butyl acrylate in a hexical fluoropolymer (PTFE, 9 mL) tubular reactor has been studied although mainly to determine

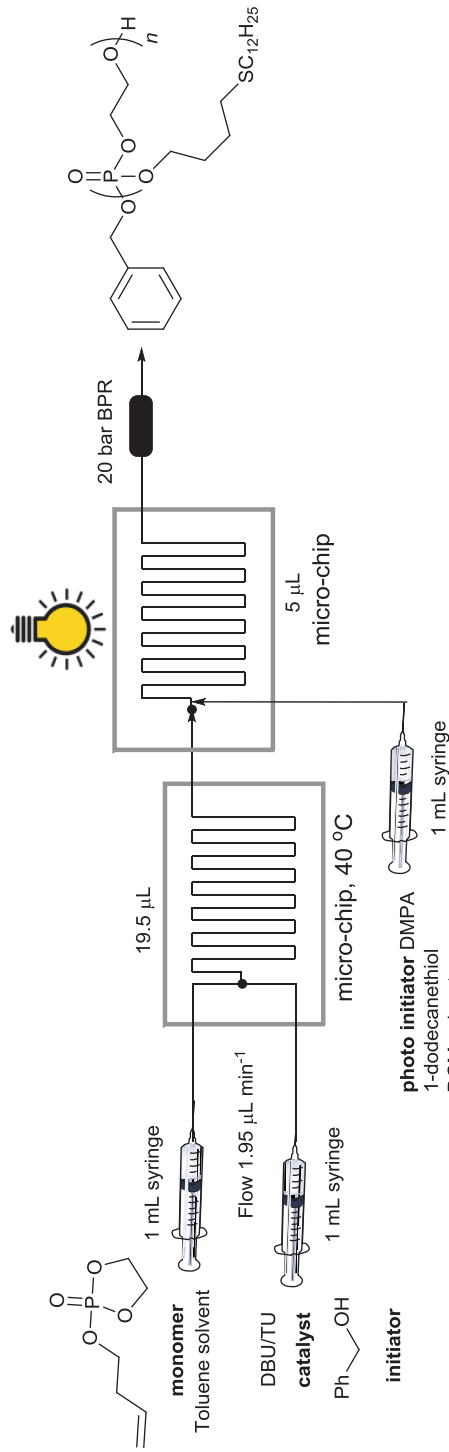

Figure 8.15 Anionic ring-opening polymerisation and UV-promoted conjugation in flow.

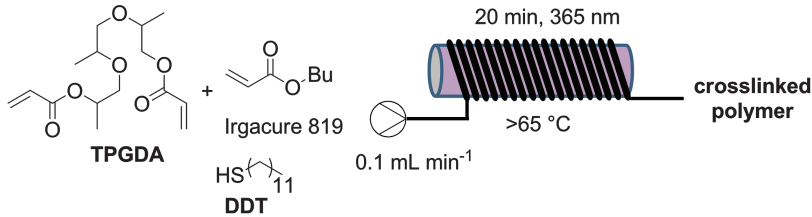

Figure 8.16 UV-promoted branched polymer synthesis in flow.

Table 8.6 Polymerisation of *n*-butyl acrylate (*n*BA) in flow and batch for different monomer to chain transfer agent molar ratios.[a]

*n*BA	TPGDA	DDT	Method	Conversion (%)	M_n (g mol^{-1})	M_w (g mol^{-1})
60	1	5	Batch	99	2100	5800
60	1	5	Flow	71	2300	5500
60	1	3	Batch	96	3400	14 400
60	1	3	Flow	74	3900	12 000
60	1	2	Batch	96	6200	78 000
60	1	2	Flow	76	6700	61 500
60	1	1	Batch	73[b]	12 300	109 000
60	1	1	Flow	78	14 000	140 000

[a] M_n molecular weight and M_w determined by SEC. Conversion of the monomer as determined by ^{1}H-NMR.
[b] After only 8 min of irradiation.

the critical parameters that most influence the occurrence of reactor blockage.[44] These were shown to be solid content >30 wt%, surfactant concentrations <1 wt% and a tubing diameter <1 mm internal diameter. The reactor used for the investigation comprised the PTFE coil spiralled around a quartz cylinder (60 mm o.d. 400 mm length) into which an 18 W black fluorescent light (350–410 nm) was inserted. A stock solution of the emulsion was prepared and fed into the reactor. The steady state acrylate latex output (average particle diameter 80 nm and $M_n = 103$ kDa) was stable to coalescence and Ostwald ripening. Although not well evidentially supported adhesional wetting was forwarded as the main triggering event leading to clogging of this reactor system.

The conceptualisation of CRP and development of ATRP was a significant and revolutionising invention that redefined the area of polymer chemistry and led the way to later modifications such as SET-LRP and SARA-ATRP[45] (supplemental activator and reducing agent). Although several transition metals have shown great promise, the area has been dominated by the use of copper. Several approaches have been applied with the aim of reducing the copper concentration with photochemistry gaining special attention due to the temporal-spatial resolution and its simple application at ambient temperatures.

Chuang *et al.*[46] applied photo-CMP towards multi-block co-polymer synthesis under flow under flow processing conditions. Block copolymers

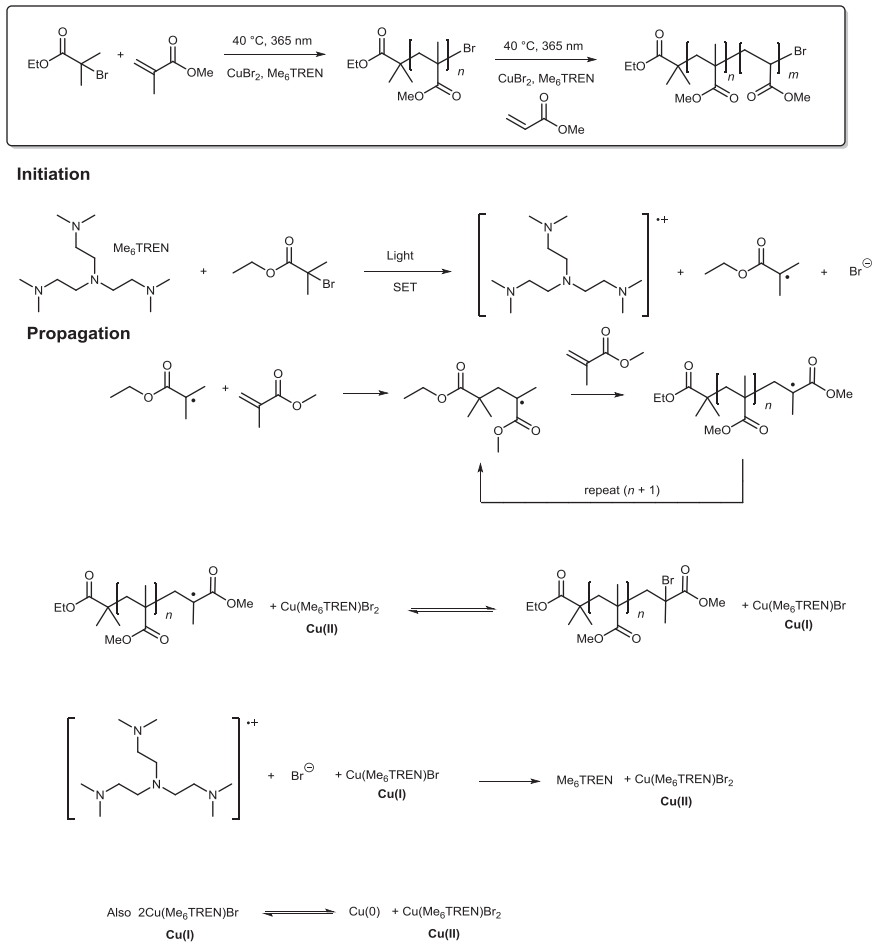

Figure 8.17 UV-induced copper-mediated synthesis of PMMA-*b*-PMA-Br co-polymer and mechanism.

containing poly(methyl acrylate) (PMA) and poly(methyl methacrylate) (PMMA) (Figure 8.17). A tubular flow reactor was prepared by wrapping a 25 m length of fluorinated tubing (0.75 mm ID) around a quartz glass tube core into which a 15 W light source was inserted (peak emission 365 nm). An HPLC pump was used to drive the solution through the reactor coil to be collected into a glass vial containing a hydroquinone quench solution. Under the flow conditions the polymerisation of MMA reached ~50% within 60 min residence time which was three times greater than achieved in batch being indicative of the better photon penetration. However, it was noted that $Đ$ increased in flow. After isolation of the PMMA–Br ($M_n = 2600$ g mol^{-1}, $Đ = 1.30$) it was subjected to a second polymerisation with MA to form a PMMA-*b*-PMA-Br co-polymer of different final M_n by using different residence times (Table 8.7).

Table 8.7 PMMA-*b*-PMA-Br co-polymer data.[a]

Residence time (min)	M_n (g mol^{-1})	$Đ$
10	3100	1.26
20	5300	1.23
30	5700	1.29

[a]M_n molecular weight and M_w determined by SEC.

Using this technique high precision polymers have been obtained.[47] Junkers *et al.* recently published a paper describing their efforts in the area of photo-polymerisation.[48] A photo-induced copper mediated radical polymerisation (UV SET-LRP) of methyl acrylate was conducted in DMSO at a reaction temperature of 15 °C (Figure 8.18).

The photo-polymerisation was performed in both a tubular milli-flow reactor and a glass chip fabricated micro reactor (Figure 8.19). The reaction time reported using the milli-flow reactor was much shorter than for comparative batch experiments. A residence time of only 20 min (90 min batch) resulted in high conversions of the monomer (>90%). Due to the short residence time and consequently much reduced irradiation time, photo induced side reactions were also minimised. It was stated that the increase in polymerisation rate resulted from enhanced light absorption and also the use of a more powerful UV-lamp (3.0 mW cm^{-2} *versus* 400 W medium pressure, $\lambda_{max} = 365$ nm). However, it is hard to compare the light sources and, therefore, the results of the polymerisations due to limited information in the publication. A low dispersity was achieved which dropped from 1.3 to 1.1 when higher monomer conversion and longer residence times were used. Increasing the monomer to initiator ratio resulted in higher initial dispersities. A drop in dispersity was noticed at 40% conversion and a second drop at 60% conversion. All target molecular weights investigated (2000, 4000 and 9800 g mol^{-1}) yielded a similar trend. To access the specific target molecular weights, different ratios of monomer and initiator were used (c_{mon}/c_{init}), 23, 47 and 116 respectively. Unfortunately, the target molecular weights were not achieved but the reason for this was unclear (Table 8.8). For comparison, batch polymerisations under equivalent conditions gave dispersity in the range of $Đ = 1.11$ to 1.05, with consistent molecular weight to the polymers synthesised in the tubular reactor.[49]

The same UV SET-LRP reaction of methyl acrylate was also performed in a micro-flow device (Figure 8.19). A M_n of 4 kg mol^{-1} was targeted and a maximum conversion of 80% was achieved with a residence time of 20 min. The produced polymers had similar average molecular weight and dispersity for the polymerisations performed in the micro-flow reactor and the milli-flow reactor. The results were used to scale up the polymerisation, the described set-up was able to produce approximately 60 g of polymer per day in the tubular reactor. The PFA tubing (1/16″ × 0.75 mm, $V_{tubing} = 11$ mL) was wrapped tightly around a UV-lamp (400 W medium pressure, $\lambda_{max} = 365$ nm), and an HPLC pump was used to deliver the reaction mixture.

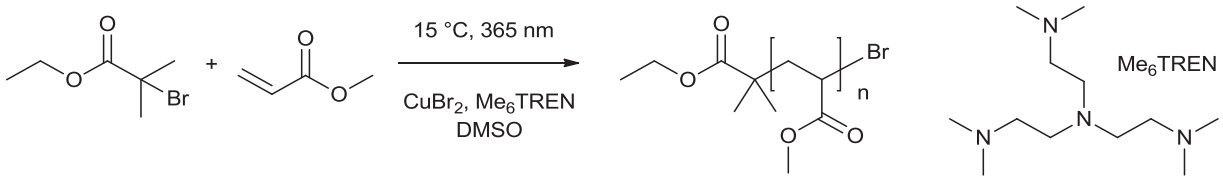

Figure 8.18 UV-induced copper-mediated polymerisation of methyl acrylate.

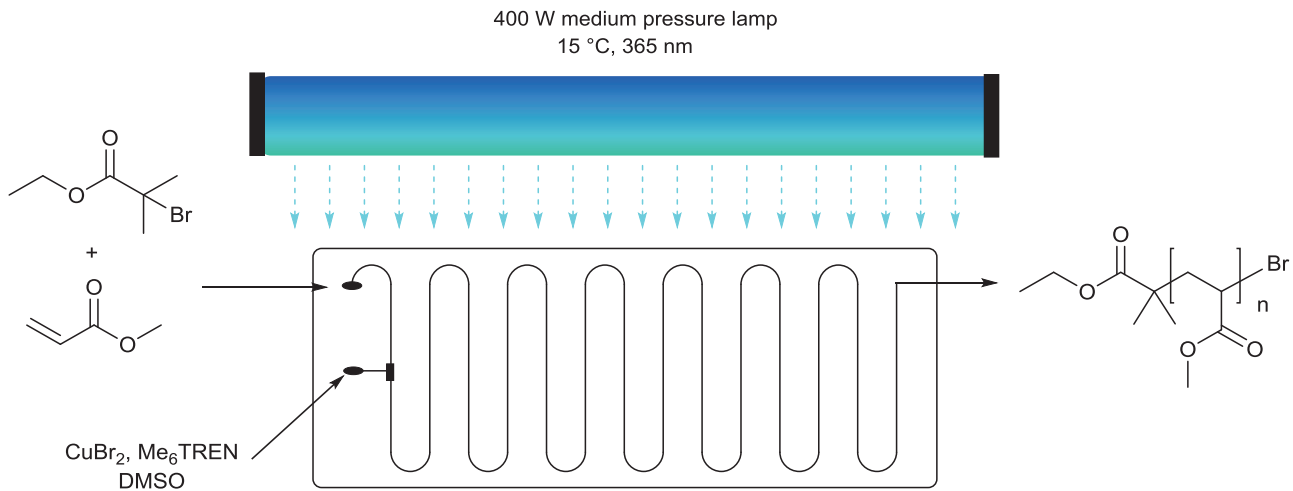

Figure 8.19 Micro-flow UV SET-LRP reaction of methyl acrylate.

Table 8.8 Targeted and obtained molecular weight.

	Target M_w ($g\,mol^{-1}$)	Approximate obtained M_w ($g\,mol^{-1}$)	Conversion (%)
1	2000	1550	86
2	4000	2600	78
3	9800	500	68

Block co-polymerisation of methyl acrylate and butyl acrylate was also performed using the same micro-flow set-up (Figure 8.19). First methyl acrylate was polymerised ($M_n = 3100\ g\,mol^{-1}$, $Đ = 1.10$). Next, the butyl acrylate was copolymerised with the active poly(methyl acrylate) chains with a M_n of 7700 $g\,mol^{-1}$ being formed if full conversion of butyl acrylate was obtained. Good control over the polymerisation was achieved, with a dispersity of 1.16 and a number average molecular weight of 4990 $g\,mol^{-1}$ at was for a conversion of butyl acrylate of 51%. This indicates a corresponding theoretical M_n of 5400 $g\,mol^{-1}$. To extend the scope other monomers were tested. Previous batch polymerisations had shown a large variety of monomers could be used to form block co-polymers using copper mediated photopolymerisation. However, not all monomers tested gave good results for block co-polymerisation in flow. Attempts to prepare a block co-polymer of poly(methyl acrylate) with styrene, for instance, did not show significant secondary polymerisation, where methyl methacrylate gave a poor conversion (35%) beyond 20 min ($M_n = 2100\ g\,mol^{-1}$, $Đ = 1.45$). The reaction times were not extended above 20 min. It is known that methyl methacrylate is harder to polymerise due to the stability of the intermediate radical. Therefore, extended reaction time could increase the conversion.

The 10-phenylphenothiazine organocatalyzed photo-ATRP of methacrylic acid has been studied by Ramakers *et al.*[50] in which first a general set of reaction conditions for the process were generated in batch and then transferred and adjusted for operation under flow. This was required due to the improved light efficiency which resulted in generally faster kinetics and thus shorter reaction times using the flow reactor. Unfortunately, it was indicated that the higher photon irradiation can also lead to loss of the end groups especially under longer residence times meaning reaching high monomer conversion was problematic.

The development of photoinduced electron/energy transfer-reversible addition–fragmentation chain transfer (PET-RAFT) polymerisation[51] has allowed the exploitation of visible light to gain greater control over the polymerisation process.[52] Corrigan *et al.* have investigated the preparation of acrylamide polymers using a photo flow reactor. The set-up consisted of a series of LED strips (60 LEDs per meter, green 530 nm) which were attached to the inner wall of a large (15 cm ID) poly(vinyl chloride) pipe. A second insert made from transparent PMMA pipe (10 cm o.d.) was used to hold and position a spiral of FEP flow tubing (1/16″ ID, total volume ~ 600 μL) around through which the reaction mixture was flowed.[52,53] When using DEAm or

DMAm, with the RAFT agent DTPA, and porphine derived photocatalyst ZnTPP (50 ppm, Figure 8.20) in DMSO, as the solvent, produced polymers all of which displayed very narrow and unimodal molecular weight distributions in 30–90 min residence times. Furthermore, it was shown that by changing the wavelength from the starting 530 nm (green) to 630 nm (red) or 460 nm (blue), whilst maintaining the light intensity (1.4 W m^{-2}) also led to different monomer conversions and new polymers with differing degrees of polymerisation, and different M_w (Table 8.9).

The same research group have recently reported an extension of their photo flow RAFT synthesis of gradient polymers (again using ZnTPP photocatalyst; Figure 8.20) by adding a subsequent controlled chain extension.[54] A two stage reactor allowing sequential injection of the reacting monomers enabled a wide range of tailored mixed polymers with different molecular weights to be prepared (Figure 8.21). A high correlation between predicted and experimental molecular weight distributions was found enabling the reactor to be used to generate precision polymer output on demand.

The immobilisation of a tetraphenylporphyrin (TPP) photocatalyst to the surface of cotton threads *via* a triazine linker has recently been realised.[55] The resulting heterogeneous system was used to instigate photoinduced chain transfer polymerisation (PET-RAFT polymerisation) of *N,N*-dimethylacrylamide (DMAm) in a flow reactor. The photocatalyst fibres (~4 m length) was folded and threaded through an FEP tube (35 cm length) and a stock solution of DMA and 2-cyano-2-propyl dodecyltrithiocarbonate (CPDTC) as the RAFT agent pumped through at a flow rate of 1.93 μL min^{-1} enabling a

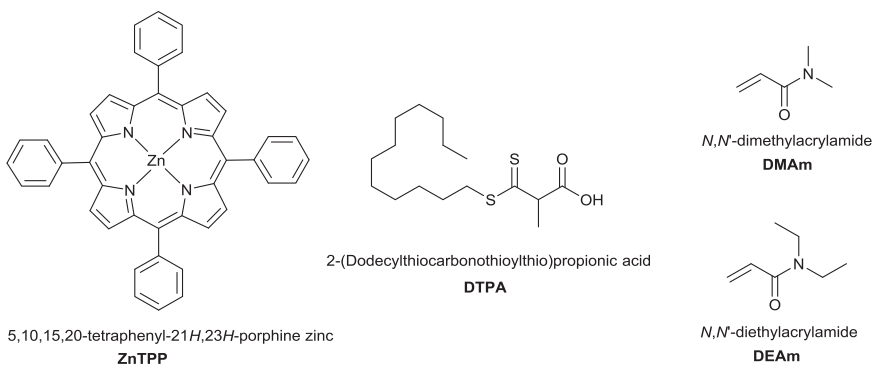

Figure 8.20 PET-RAFT polymerisation of acrylate and acrylamide.

Table 8.9 Polymers produced from DMAm under different wavelengths at a fixed 90 min residence time and light intensity of 1.4 W m^{-2}.

	λ (nm)	Conversion (%)	Target M_w (g mol^{-1})	$Đ$
1	460	57	28 600	1.10
2	530	79	38 400	1.12
3	630	71	33 600	1.09

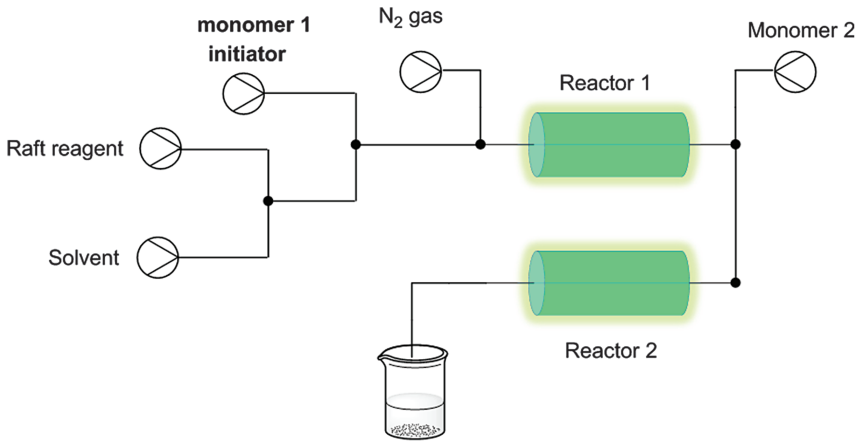

Figure 8.21 Two stage sequential reactor for photocatalysed polymerisation.

10 h residence time under irradiation with green light ($\lambda_{max} = 530$ nm, 0.45 mW cm^2) (Figure 8.22). A consistent monomer conversion of 65% was achieved for over a 20 h run producing a polymer of M_n in line with the theoretically calculated (figure not given in the paper) and a PDI > 1.20. This simple catalyst immobilisation could be used in many other applications.

8.3 Enzymatic Polymerisation

Only a few papers have been published on the subject of enzymatic polymerisations in flow although this is an area which is set to become a new high impact area especially for the preparation of new biodegradable polymers and chiral polymers.

One example disclosed by Bhangle *et al.* described the synthesis of polycaprolactone from ε-caprolactone.[56] The enzyme *Candida Antarctica* Lipase B (*CAL B*) was immobilised on solid beads (macroporous polymethyl methacrylate) and packed into a column reactor which enabled a higher local concentration than could be achievable in batch. Although good performance was demonstrated at lab scale the reactor set-up was not deemed suitable for scale-up due to its small volume. The residence time range was short (15–240 s) and the flow rate coverage low (30–640 μL min^{-1}).

The same group later went on to evolve their reactor design to create an enzyme packed microreactor where the internal capillary channels of the chip based system were filled with the immobilised *CAL B* (Figure 8.23).[57] The apparent rate constant in the microreactor was >27 times larger than in batch. A series of pseudo-dry and water saturation conditions were tested to determine the impact on the rate of the polymerisation reaction and also degree of retention of the benzyl ester end groups. Improved results were found for the microreactor compared to the batch comparison.

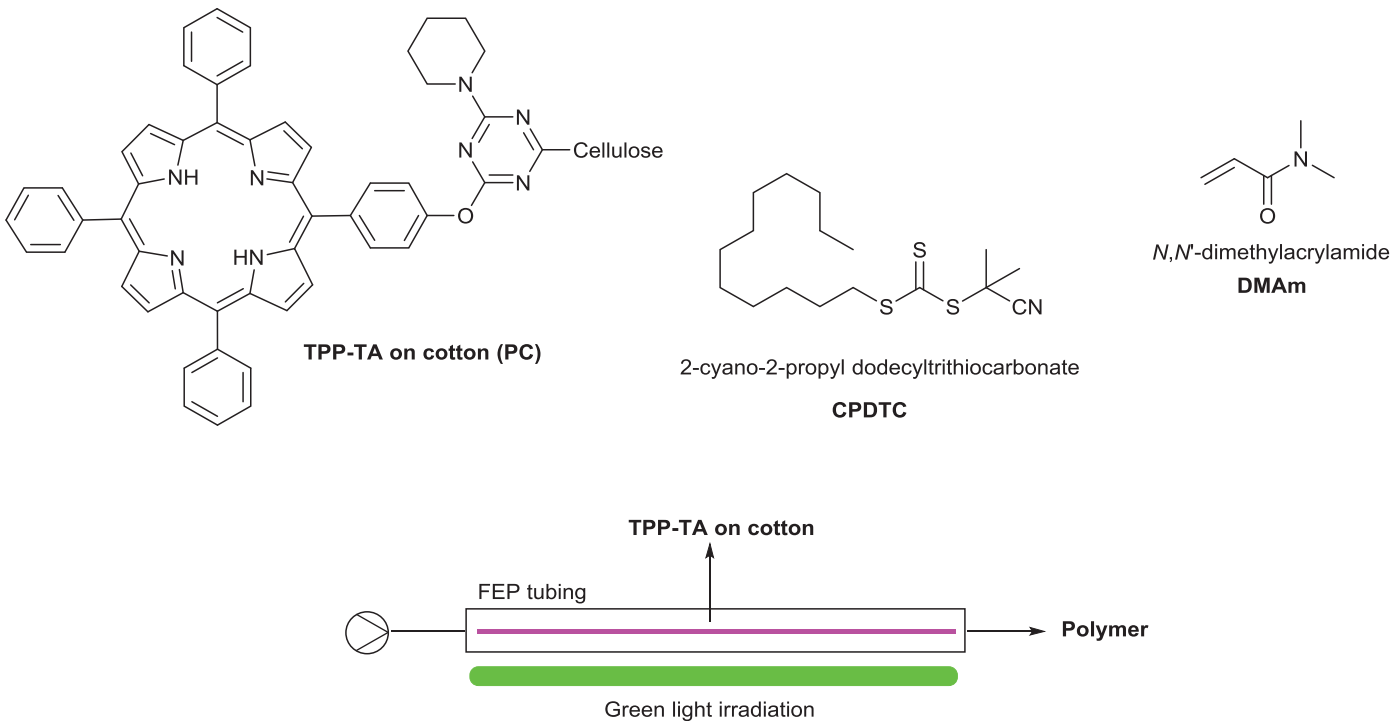

Figure 8.22 Flow PET-RAFT polymerisation of *N*,*N*-dimethylacrylamide.

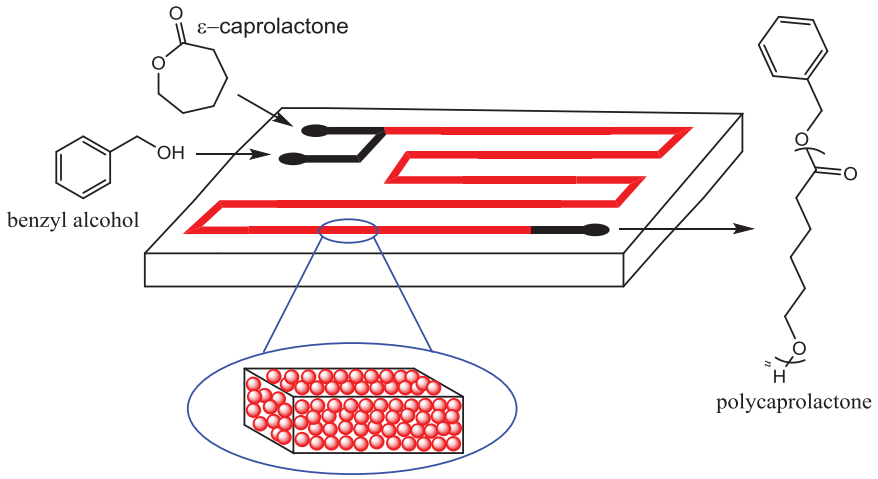

Figure 8.23 Enzyme filled capillary channel reactor.

Zhang *et al.* returned to the use of a packed bed reactor involving a self-prepared immobilized lipase (Lipase from *Candida* sp.).[58] Interestingly, as well as evaluating the standard parameters expected to affect the poly(ε-caprolactone) (PCL) production such as residence time and monomer concentration (0.2–2.25 mol L^{-1}) the height to diameter (*H*/*D*) of the packed column was also investigated. As this can impact the contact time between the enzyme and the reactants this might have a significant impact on the reaction outcome. The reactor column was thus filled with varying quantities 0.5–2.5 g of immobilized enzyme to contrast the height from 4 to 20 cm (1 cm ID). There are two competing catalysed reactions to the polymerisation and potential degradation rate. It was found that when the *H*/*D* ratio increased from 4.0–12.0, the polymerisation rate increased. However, when the *H*/*D* ratio > 12.0, the polymerisation rate increased slower than the degradation rate, and thus the molecular mass of PCL decreased. Therefore, a fixed *H*/*D* ratio of 12 was set for the investigation. In general it was also found that monomer conversion increased with residence time, to reach a maximum (>98%) at 12 min. The M_n of PCL attained was 15.6 kg mol^{-1} with a dispersity index of 2.1 and the system could be successfully run over 460 h achieving a PCL productivity of 19.15 g g^{-1}(enzyme) day^{-1}.

Further to this work, the use of Novozym 435 in a packed bed reactor for application as a flow process has been patented, however, several details of this work are hard to decipher from the presented content.[59]

Very recently Zhu *et al.* showed that an enzymatic flow synthesis of thiol terminated poly(δ-valerolactone) could be acheived.[60] The immobilised enzyme (1.16 g; CALB; 10 wt%, 0.3–0.9 mm beads) was loaded into a PTFE tube (3.8 mm ID × 300 mm length) to create a residence volume of 1.8 mL. The coil was submerged in an oil batch and maintained at 60 °C for the duration of the reaction. A stock solution of the reactants was passed through the system with

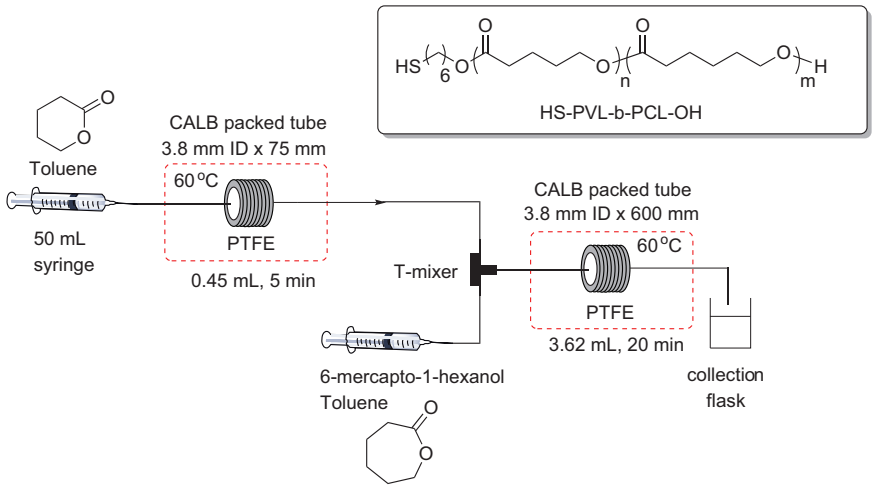

Figure 8.24 Enzymatic synthesis of thiol-terminated block-copolymer in flow.

a 20 min residence time (flow rate 0.09 mL min^{-1}) allowing 98% monomer conversion, an $M_n = 3120$ g mol^{-1} and $Đ = 1.16$ with 95% thiol fidelity. A modified dual reactor configuration also allowed block co-polymerisation to be run using sequentially linked enzymatic reactors (Figure 8.24).

8.4 Integrated Reaction Monitoring

An added advantage of flow chemistry is that work-up and purification can be linked and performed in-line, ideally as part of an integrated process. There are several literature reported examples of conducting purification and in-line analysis of small molecules, but only a limited selection of papers have approached this challenge regrading macromolecules. There are, however, known practices suitable for achieving the separation of polymeric reaction mixtures as part of a flow sequence.[61]

One possible reason for the low number of papers published relating to direct in-line analysis of polymerisation reactions might be the requirement for sample preparation prior to analysis, which is often a time consuming process. Especially if a pure sample is required for analysis (*i.e.* by GPC). It can be difficult to simply inject a sample straight from the flow line into a GPC. The sample would, at a minimum, need dilution to a known concentration and probably require filtration before injection. Alternatively, mass spectrometry could be used to determine the molecular weight, although this can become problematic for high molecular weights due to detector limitations. Alternatively, many experimenters have instead approached the problem by adopting an on-line analysis approach.

In the area of flow chemistry different terminology is often used to describe the way analysis is performed. In this thesis we will use three different

Table 8.10 Characteristics of off-line, on-line and in-line analysis.

Process analysing	Sampling method	Sample transport	Analysis
Off-line	Manual	Remote	Automated
Off-line	Manual	Remote	Manual
On-line	Automated	Integrated	Automated
In-line	Integrated	No transport	Automated

terms: off-line, on-line and in-line analysis. The characteristics are described in Table 8.10.[62]

To make effective use of combinatorial and high-throughput approaches to the discovery of new polymers with unique molecular and physical properties requires the co-development of associated rapid analytics in order to not create an analysis bottle-neck. Hoogenboom *et al.*[63] have assessed the use of GPC and gas chromatography (GC) analysis as integrated parts of an automated synthesizer for polymer preparation. This enabled an accelerated work flow (synthesis–analysis–assessment–resynthesis).

Indeed, several other valuable direct sampling processes have been reported for diagnostic on-line analysis of progressing polymerisation reactions. For example a MALDI-TOF MS system has been built for cationic ROP (CROP) of 2-ethyl-2-oxazoline which used a xyz-liquid handling system to sample and add aliquots directly onto a MALDI target.[64] On-line GPC characterisation of ATRP polymer samples have been automatically processed involving filtration through short aluminium oxide columns to sequester the copper salts prior to direct analysis has been shown.[65] On-line GPC has also been performed by Reed *et al.*[66] using the automatic continuous on-line monitoring of polymerisation reactions (ACOMP) system. This system was again based on batch reactor system with continuous sampling. It allowed measurement of the developing average molar mass, intrinsic viscosity and monomer conversion kinetics. Furthermore, in cases of co-polymerisation ACOMP enabled assessment of average composition drift and distribution. Dielectric measurement offers a very simple and non-destructive method for determining the progress of polymerisation reactions.[67] The high temperature (100 °C) ROP of ε-caprolactone has been successfully monitored providing a calibrated measure of monomer conversion. Similarly, IR spectroscopy has also shown great potential as a tool for the on-line assessment of monomer conversion.[68–71] Another interesting technique has been to employ a flow cell bench top NMR as a sensitive online detector for SEC.[72] Two homopolymers polymethylmethacrylate (PMMA) and polystyrene (PS) and a branched species were assessed demonstrating a wealth of information rich spectra that could be obtained regarding the polymers composition. All of these techniques offer tremendous value and options for easily coupling them to the end or as in-line tools for flow reactors are becoming increasingly possible.

A demonstration of the use of in-line analysis and purification was reported by Hornung *et al.* based upon the aminolysis of the end group

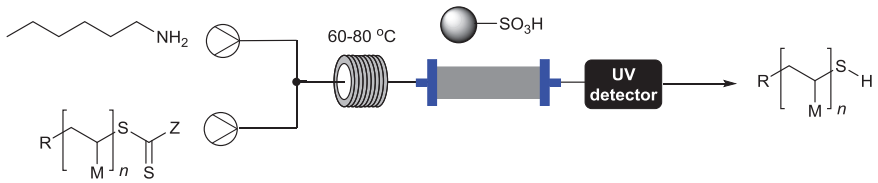

Figure 8.25 UV-monitoring of the aminolysis of the end group functionalities of RAFT polymers.

functionalities of RAFT polymers into a corresponding thiol or thioether.[73] The aminolysis of the end groups was followed using in-line UV spectroscopy (Figure 8.25). Residual monomer impurities could act as a Michael acceptor in the aminolysis allowing for the elimination of the thiol (intermediate of reaction with hexylamine). To prevent formation of the potential disulfide by-product a polymer supported packed column of Amberlite IR-120 (particle size: 300–1180 μm, 14–52 mesh) was placed in-line after the aminolysis reactor to scavenge the excess hexylamine.

Bally *et al.*[74] constructed a fully assimilated mini-flow plant for continuous processing of monomers directly through to polymer nanoparticles. Their plant integrated three main stages involving the polymerisation reaction, polymer analysis and nanoparticle formation into a single sequence (Figure 8.26).

First, linear and branched polymethacrylates/vinyl copolymers were synthesised *via* ATRP in the tubular flow reactor where the polymer properties could be tuned by changing the reaction parameters (reagent ratios, flow rate, temperature) to generate M_n ranging from 2–20 kg mol^{-1} (0%–5% branching). In the analysis stage, multi-detection GPC allowed monitoring of molecular weight distribution over time, and the easy identification of the establishment of steady state reactor operation. Finally, isolation of the polymer was achieved by nano-precipitation, this step also facilitates the simultaneous purification of the polymer through its separation from the soluble residual monomer and catalyst. Micromixers are used to produce a colloidal suspension of the diluted polymer which is further mixed with a precipitating medium (non-solvent–water) furnishing the polymer nanoparticles with diameters ranging from 89–196 nm (average size distribution 41 nm). As each stage of the process is fully adjustable it becomes possible to program for different nanoparticle sizes and compositions with the future aim of looking at encapsulation of pharmaceuticals.

On-line monitoring of the RAFT polymerisation of *n*BA, using 2-(dodecylthiocarbonothioylthio)propionic acid (DoPAT) and 2-2′-azoisobutyronitrile (AIBN) as the thermal initiator (Figure 8.27) was performed by Junkers *et al.*[75] An electrospray ionisation mass spectrometry (ESI-MS) was coupled with a Labtrix Start R2.2 system. The reactor was a glass microchip with an internal volume of 19.5 μL meaning rapid reaction changes could be made. A variety of molecular weight polymers were obtained. At 100 °C molecular weights of 1100–2700 g mol^{-1} were obtained for residence times between 1 and 5 min. The direct monitoring *via* mass spectroscopy allowed

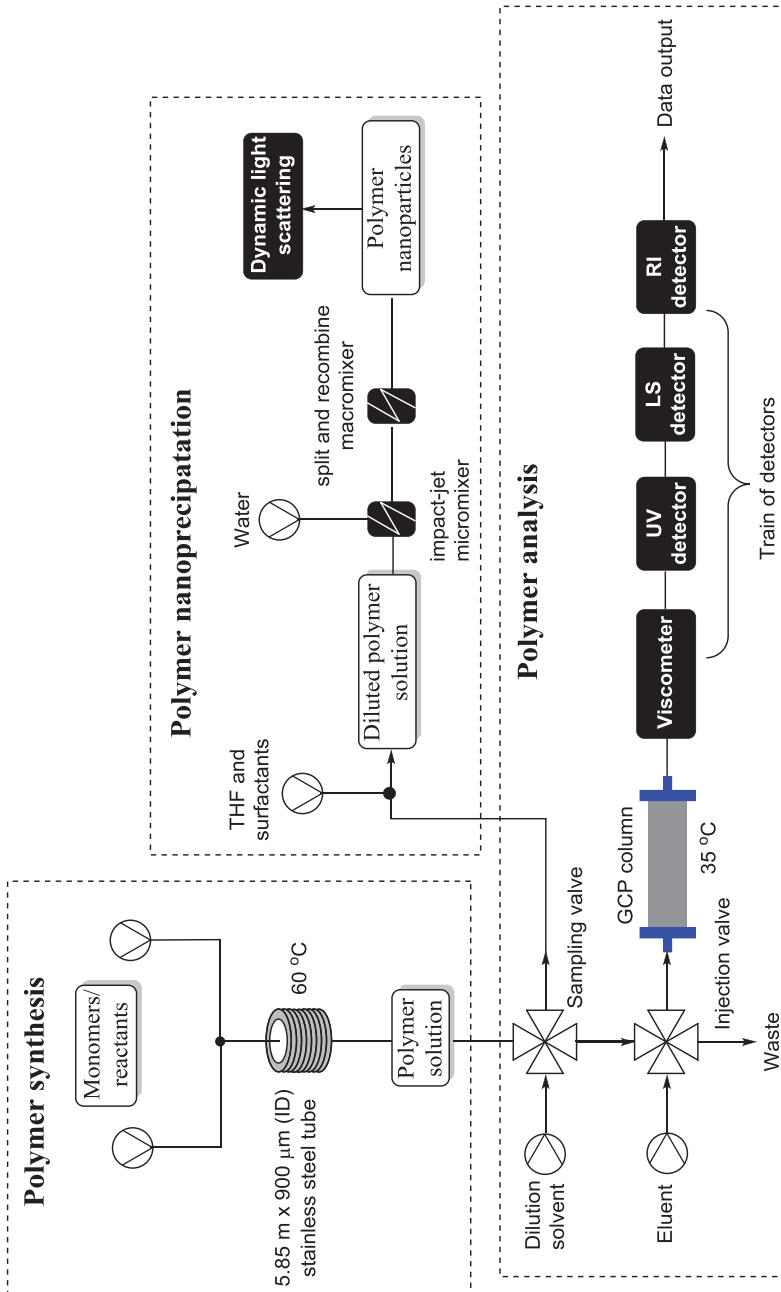

Figure 8.26 Schematic of the mini-nanoparticle plant.

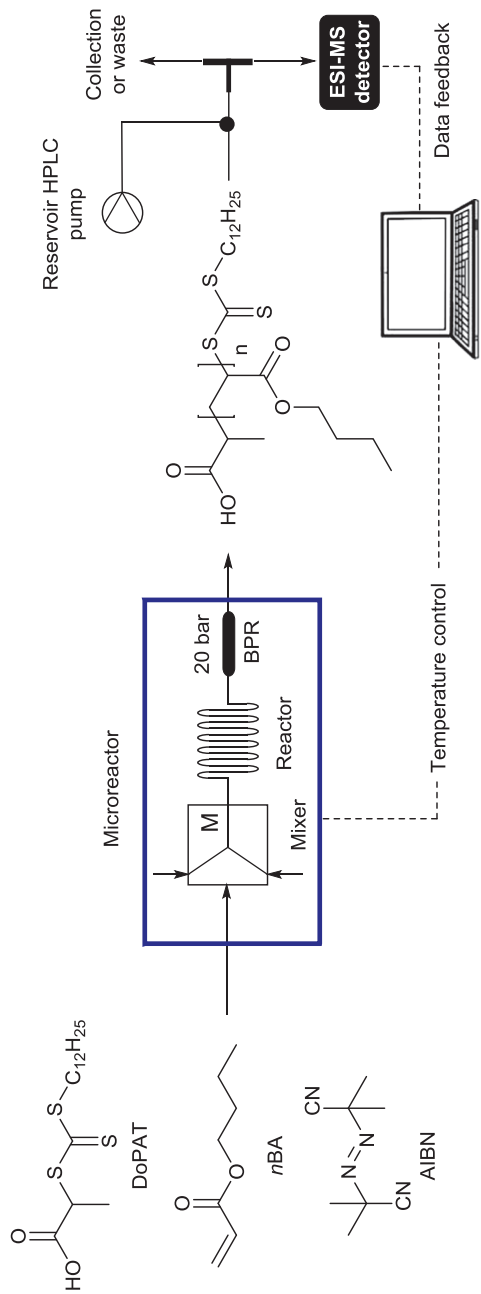

Figure 8.27 RAFT polymerisation for on-line monitoring.

the viewing of the polymer growth by fitting the time profile of the reactor with the MS data obtained giving essentially a real time response. This allowed changes to be made and within minutes information could be gathered regarding the effect on the polymers being produced. It was, therefore, possible to correlate the output with changes in temperature and to create direct feedback loops for optimisation.

The Cu(0) catalysed polymerisation of methyl acrylate (MA) *via* SET-LRP process has been monitored in real time to obtain conversion and molecular weight distribution data without the necessity of manual sampling (Figure 8.28).[76] The system utilised GPC analysis (3 min run time) coupled with low angle laser light scattering detection to provide polymer characterisation data whilst changes in active $CuBr_2$ concentration were monitored on-line using a photodiode array detector.

The rapid analysis of the data allowed the kinetics of the process as well as key attributes of the polymerisation to be determined. For example, the selection of solvent, ligand and additives were shown to be critical to the success of the polymerisation. A polar/coordinating additive (phenol/alcohol) and the presence of *N*-donor ligands (Me_6TREN) promote the disproportionation of Cu(I) to Cu(0), the proposed active species in SET-LRP. The toluene solvent ensures full solubility of the monomer and polymeric product. Although the polymerisation was performed in CSTR the monitoring was fully automated and indicates how a more integrated flow solution could be constructed.

More recently, Rubens *et al.* have developed these ideas of reaction monitoring and automation to create a platform capable of autonomous self-optimisation of polymers in flow.[77] A computer controlled unit integrates a flow reactor unit with a SEC allowing direct on-line molecular weight distribution measurements which are used by machine learning algorithms to optimise the reactor to generate polymers towards pre-programmed molecular weights. The system has proven highly skilled at reproducibly targeting precise molecular weight (<2.5% deviation from a preselected target). Currently the system has been used for RAFT polymerisation of *n*-butyl acrylate but is anticipated that it could be used for other more challenging polymerisation reactions.

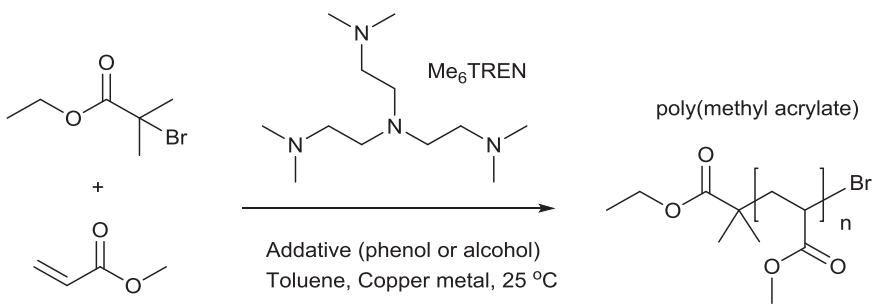

Figure 8.28 SET-LRP of methyl acrylate (MA).

8.5 Polymer Purification

The purification of a newly synthesised polymer can often be the slowest step in the sequence of converting monomer to polymer and obtaining analysis. The method selected to purify a polymer is highly dependent on several factors such as the polymerisation technique used, the resulting chemical structure of the polymer and critically the final specification and application of the polymer. For some applications, a very high purity is required, such as in medicinal applications[78] or organic photovoltaic devices.[79] Other applications, such as thickeners or food packaging do not necessarily require polymers possessing such narrow dispersity but may need exhaustive removal of any residual monomers.

In general, polymers can be separated from the reagents (residual monomer(s), catalyst, *etc.*) but can also be separated by molecular size. Polymers with various molecular weights can be sorted/separated, using membranes with different pore molecular weight cut-offs.[80] To perform analysis, it is preferable to have a clean sample, often of monomodal dispersity especially for GPC analysis. A central aspiration of polymer chemistry in recent years has been greater automation so that a reaction performed at laboratory scale could be screened, purified and analysed directly in-line or on-line and the data evaluated to enable a rapid improved secondary synthesis.[74,81,82] This fits nicely with flow processing where the ability to both monitor the reaction and directly effect change to the processing conditions in essentially real time becomes very advantageous.

As already described (Section 8.4) although polymer synthesis has benefited from several in-line real time monitoring techniques (*e.g.* example, IR and Raman spectroscopy[83]), until very recently,[76,77] polymer synthesis had not been performed in a system containing in-line or on-line GPC analysis for the determination of molecular weight and dispersity in combination with flow chemistry.

8.5.1 A Brief Review of Purification Techniques

8.5.1.1 Anti-solvent

One way of purifying a polymer sample is to find a solvent or solvent mixture in which either the residual monomer or resultant polymer is soluble but the other component is not. This methodology is probably most preferred, especially at an industrial scale, as it is the easiest to perform. Ideally, the polymer component would precipitate but it may also form a gel. It should be acknowledged that the addition of certain solvents (anti-solvents) can add issues relating to contamination depending on the specific application (*i.e.* medical). In addition, it is often difficult to be selective regarding molecular weight cut-off in terms of precipitation methods and yields of recovered material can be variable. Controlled precipitation has been more used in flow for preparing nanoparticles and for encapsulation processes.

8.5.1.2 Dialysis

The principle of dialysis is based upon diffusion of material from a high concentration zone to an area of low concentration across a semi-porous membrane.[84] Unfortunately, not all polymerisation reactions can be purified using dialysis. The challenge is finding tubing or membranes that are compatible with the full range of organic solvents or polymers produced. Despite this, as a technique it has been shown to be a viable for the efficient purification of a broad range of natural products such as enzymes,[85,86] proteins,[86,87] polysaccharides,[88] lignin sulfonates,[89] polymers in semi-aqueous systems[90–92] and polymers in aqueous systems.[93] Alternatively, and for a completely different application, dialysis tubing has been used to grow bacteria as described by Millner *et al.* where nutrients and by-products could pass through the tubing.[94] All of the above applications have one thing in common: that the purifications are (partly) performed in water. Residual monomer and reagents (especially inorganic compounds) are readily removed from the solutions by transport across the semipermeable membrane. The strength/efficiency of the dialysis varies with the surface area and pore size of the membrane. Dialysis membranes are generally made of regenerated cellulose, cellulose acetate, polysulfone, polyethersulfone or collagen. Polymers with various molecular weights can be separated by iteratively increasing the pore size of the membrane.[95] A major advantage of the use of dialysis tubing is that it has low initial investment costs, and the separations can be performed with only a beaker and the dialysis tubing (Figure 8.29).

A disadvantage of using dialysis tubing is its passive mode of action, meaning it can take a long time to purify a sample. Indeed, purification can easily take in excess of 24 h. In addition, the dialysis tubing has to be

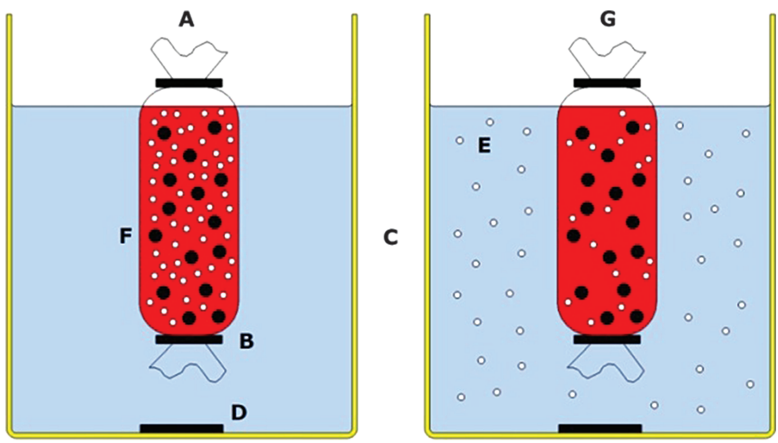

Figure 8.29 Principal of dialysis. **A:** Dialysis tubing filled with crude sample. **B:** Clips to seal the dialysis tubing. **C:** Beakers filled with solute. **D:** Stirrer bar. **E:** Small size particles. **F:** Large size particles. **G:** Dialysis tubing with purified polymer.

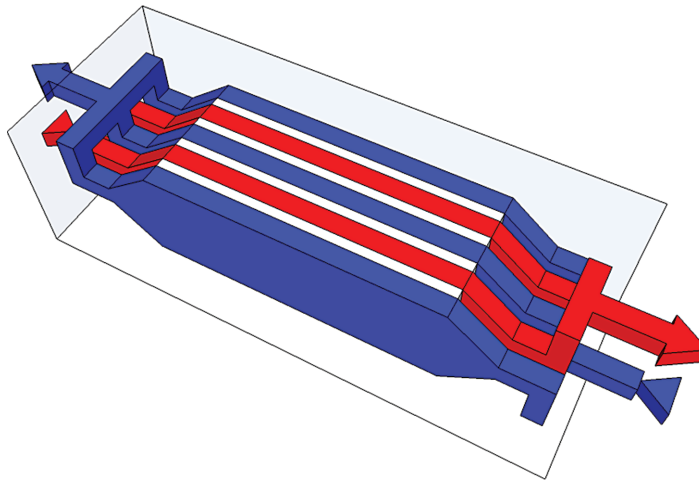

Figure 8.30 Counter-flow device, the membranes (white) separate the two flows from each other. The flow of red and blue are in opposite directions.

handled with care as the storage solutions often contain toxic compounds (*e.g.* sodium azide). Furthermore, it can be hard to process large sample volumes as it quickly becomes diluted due to the initial influx of water making the process less efficient (gradient ratios). Thus, to drive the equilibrium shifting the monomer/impurity concentration towards the bulk water source, a significant amount of water is needed. To improve the sequence, dialysis variations have been developed, such as counter-flow dialysis.[96] Counter-flow dialysis is based on the principle of two flow streams traveling in opposite directions to each other (Figure 8.30). A membrane is positioned between the streams allowing diffusion between them. Kidney dialysis is a well-known example of counter-flow purification.

8.5.1.3 Ultra-filtration

As an alternative to dialysis, ultra-filtration can be considered. There are multiple variations of ultra-filtration, for example centrifugal ultra-filtration,[97,98] and tangential/crossflow ultra-filtration.[99] In general, the advantage of ultra-filtration is that it is faster compare to dialysis *via* tubing and also includes the ability to concentrate samples. Furthermore, as with dialysis, different molecular weights can be separated as membranes with a range of molecular weight cut-off (MWCO) are available. Finally, it is also easier to recover residual monomers compared to dialysis, as the volume of filtrate is considerably smaller and therefore easy to concentrate aiding, if required, isolation and re-use. A drawback of using an ultra-filtration systems is, as with all membrane devices, the limited compatibility of the membranes with various solvents. In addition, the membranes will additionally degrade or become blocked rapidly if the sample is too concentrated as the polymer will

form clusters. To avoid this issue, a diluting solvent should be added constantly to maintain the sample's concentration which can be achieved by installing an external pump delivering the solute to the main tank with a speed similar to the withdrawal rate from the sample mixture. This balances the system and facilitates continuous throughput operation.

Brocken *et al.* utilised a commercial available Vivaflow 200 ultra-filtration system attached directly to the output of a flow reactor to purify the polymer product from free radical polymerisations of acrylic acid (Figure 8.31).[100] The aqueous soluble polymer was synthesised in water in which the residual monomer and smaller oligomers were also fully soluble. The membranes used had a surface of ~200 cm^2 and were fabricated from stabilised cellulose providing a molecular weight cut-off (MWCO) 2000 Da. A systematic study evaluating the time needed for purification was undertaken. This involved determination of the ultrafiltration set-up (path length and configuration of the multiple membranes used), flow rates (processing time) and concentrations (polymer/residual monomer). The integrated system enabled poly(acrylic acid) compositions (20–70% residual monomer, M_n 158–378 $kg\,mol^{-1}$) to be synthesised and a preparative sample purified. In all cases purification was complete in 30 min which, when added to initial synthesis time of 5–20 min, allowed a new purified polymer sample to be generated approximately every working hour.

It is sure that many other examples of such combined synthesis and polymer purification will be disclosed in the near future as the tools and sophistication of embedded automation becomes more mainstream in polymer synthesis.

8.6 Polymer Particles

An interesting and promising development area within the material sciences is the manufacture of precise polymer particles or spherical polymer capsules.[101,102] These materials are used in a wide range of products, such as drug delivery,[103] tissue replacement,[104] packaging[105] and electrochemical energy.[106] The desired properties are largely governed by their shapes, sizes and morphologies. Particles with core–shell or multi-layer structures are mainly used in coatings, spherical dielectric resonators and data storage technology. Whereas particles with liquid cores are mainly used for drug delivery, pesticides, liquid inks, paints and perfumes.[107,108] These particles are most often produced *via* controlled phase separation,[109,110] layer-by-layer deposition of polyelectrolyte multilayers,[111] interfacial polymerisation reactions[112] and Shirazu porous glass monomer emulsification accompanied by polymerisation.[113–115] Unfortunately, these methods all have drawbacks, such as expensive starting materials, time consuming procedures and in many instances the particles produced do not possess a narrow distribution or lack defined morphology. Flow chemistry has proven its strength to overcome many of these problems. Therefore, it has been utilised as a powerful technique to synthesise precise polymer particles or spherical polymer capsules.

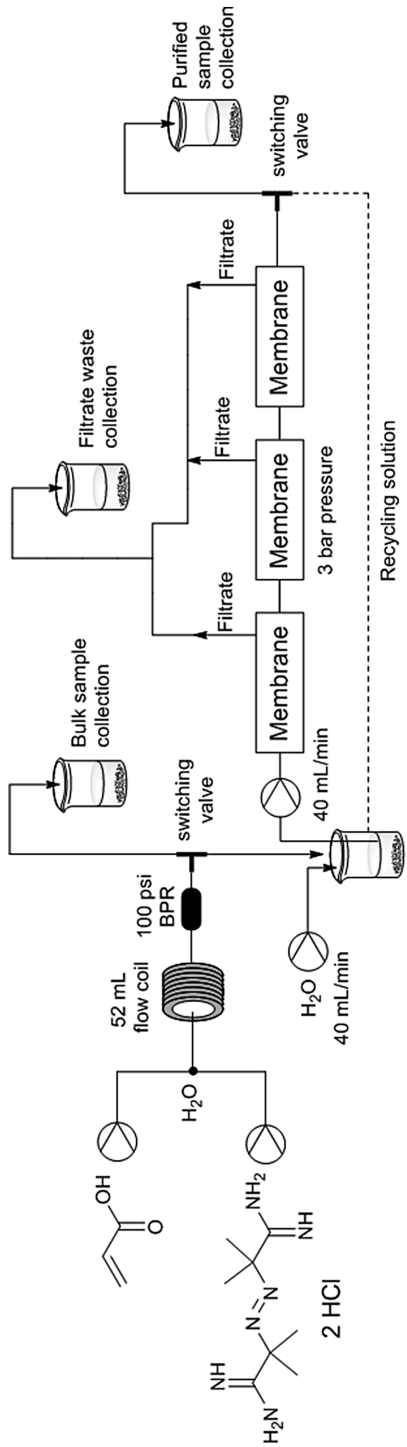

Figure 8.31 Synthesis and direct in-line purification of poly(acrylic acid).

Many different device types can be used to form droplets in flow. The two most common devices are capillary tubed and micro-structured chip based systems. The capillary-based units are mostly self-assembled bespoke reactor set-ups. The working of these devices is based on two capillaries (usually made from glass or polymer) of different outer diameters which are coaxial aligned. Using capillaries, there are two designs which are mainly used, the co-flow (Figure 8.32) and flow focussing design (Figure 8.33). The co-flow configuration has the continuous and dispersed phase flowing in the same direction. The flow focussing design has the continuous and dispersed phase flowing in opposite directions, with the output flow in the same direction as the dispersed phase.

The micro-structured chip based design can also be split into three divisions. First, a T-junction is used to mix the dispersed phase into the continuous phase (Figure 8.34). The flow rate of the dispersed phase, perpendicular to the continuous phase, will be low and the slowly growing droplet will emerge into the continuous phase and break off due to the shear forces imparted by the continuous phase. For polymeric particles a higher flow rate is used to form droplets through a higher shear force. The particles formed are smaller than the channel diameter, any droplets which are in contact with the tube will deform or stick to the reactor walls.

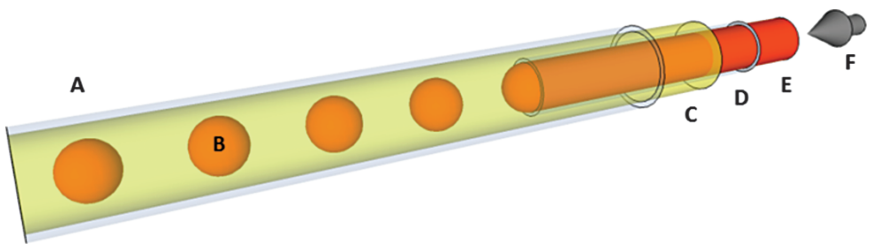

Figure 8.32 Co-flow design, **A**: outer capillary, **B**: formed droplet, **C**: continuous phase, **D**: inner capillary, **E**: dispersed phase, **F**: flow direction of continuous and dispersed phase.

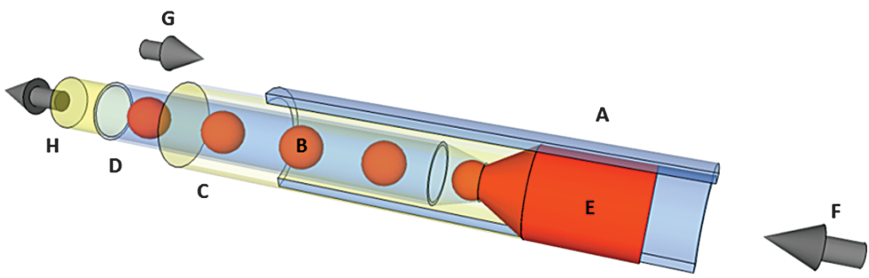

Figure 8.33 Flow focussing design with one inlet for dispersed phase, **A**: outer capillary, **B**: formed droplet, **C**: continuous phase, **D**: inner capillary, **E**: dispersed phase, **F**: flow direction dispersed phase, **G**: flow direction continuous phase, **H**: outlet of droplets and continuous phase.

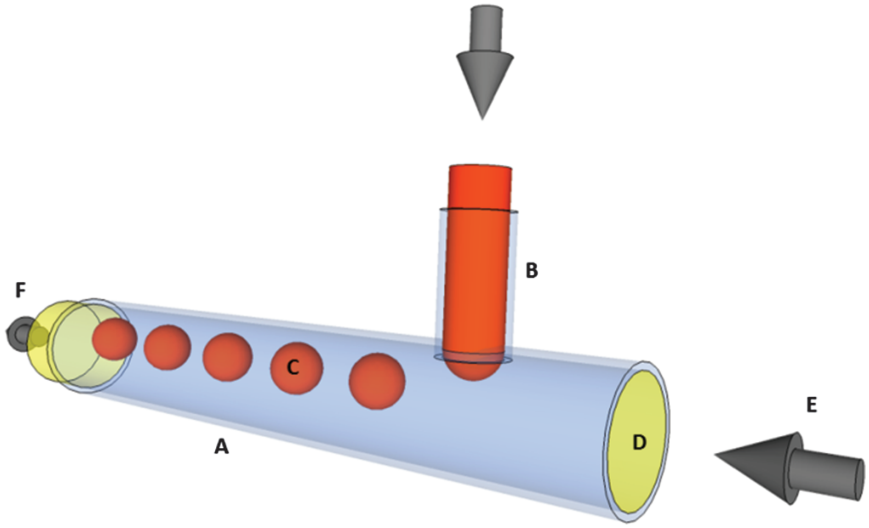

Figure 8.34 T-Junction design, **A**: capillary, **B**: dispersed phase, **C**: formed droplet, displace from equatorial position in the flow, **D**: continuous phase, **E**: inlet and flow direction of continuous phase, **F**: outlet of droplets and continuous phase.

Secondly, the use of split or intersections are also possible (Figure 8.35). A continuous phase can be introduced perpendicular to the output and added from two sides. The dispersed phase will move linearly towards the output. Consequently, the droplets will be formed by the shear force of the dispersed phase. The advantage of this approach compared to the T-junction is the alignment of the droplets. The droplets are produced more in the middle of the channel and have, as a result, less interaction with the walls. Finally, particles can be formed using flow focussing (Figure 8.36). The set-up is similar to the intersection configuration but has a narrow orifice at the exit of the channel. This set-up is most widely used as the droplets formed are of high quality.

One of the first papers describing the full continuous flow synthesis of polymeric particles was published by Kumacheva *et al.*, demonstrating the synthesis of core–shell droplets, polymer capsules and polymer particles with non-spherical shapes.[116] The paper described the importance of initially creating droplets of uniform size being the key to the whole process. This was achieved by the use of a capillary instability driven break-up of the liquid, which resulted in excellent control over the emulsification of immiscible liquids. Laminar flow streams of the three liquids (aqueous, silicon oil and monomer) were pumped through the device producing a coaxial stream of silicon oil and monomer in an aqueous phase. The control of the break-up of the coaxial liquid was important as this led to the formation of highly mono-disperse droplets (Figure 8.37).

The production of these droplets gave good control over the size of the liquid core, the thickness of the shell, the number of core droplets and the

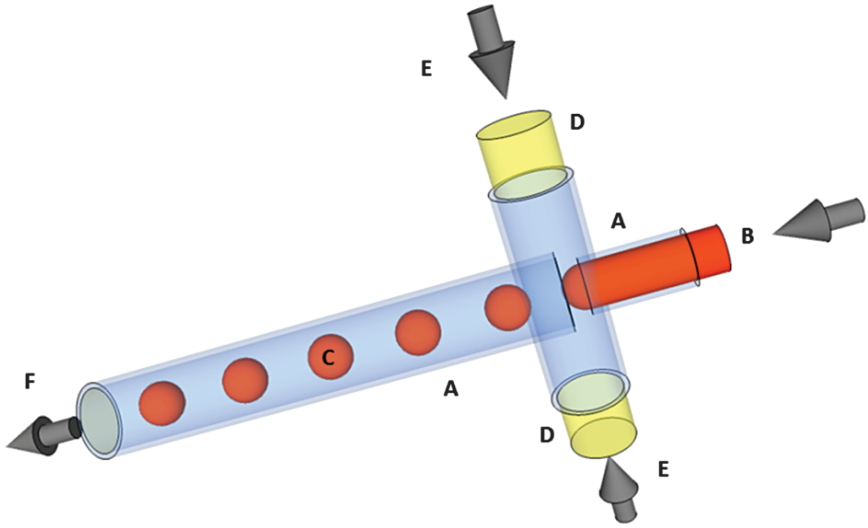

Figure 8.35 Intersection design, **A**: capillaries, **B**: inlet and flow direction dispersed phase, **C**: formed droplet, **D**: continuous phase, **E**: inlet and flow direction of dispersed phase, **F**: outlet of droplets, continuous phase and flow direction.

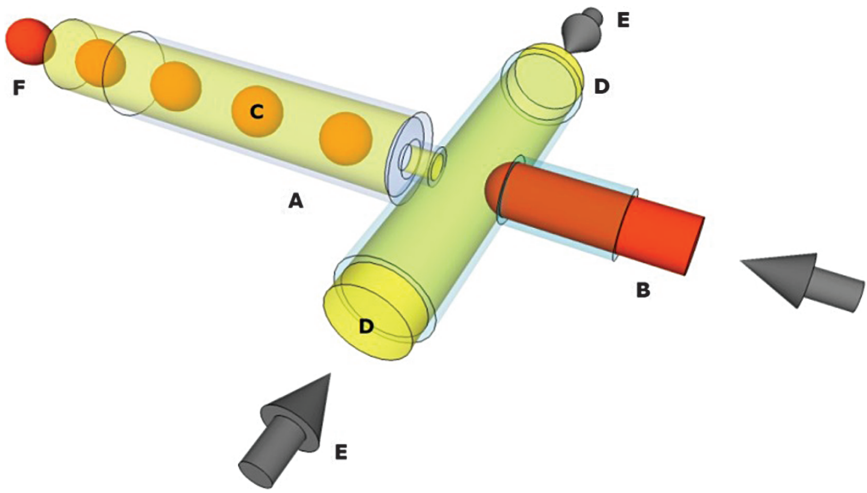

Figure 8.36 Flow focusing design with two inlets for dispersed phase, **A**: capillaries, **B**: inlet and flow direction dispersed phase, **C**: formed droplet, **D**: continuous phase, **E**: inlet and flow direction of dispersed phase, **F**: outlet of droplets, continuous phase and flow direction.

size of the particles produced. This was achieved by changing the flow rate of each liquid and maintaining the other two flow rates constant.

In the next stage the freshly prepared droplets were continuously photo-polymerised under UV irradiation (360 nm, 200 mW m^{-2} intensity at sample

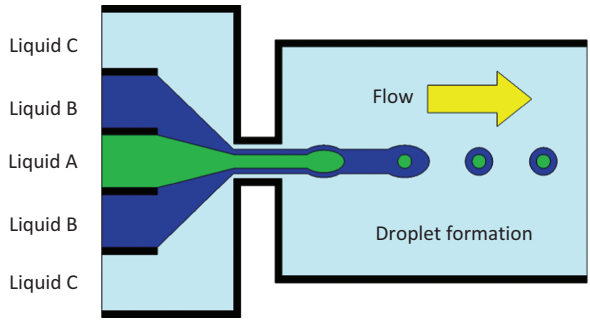

Figure 8.37 Schematic view of flow streams for the formation of droplets, laminar co-flow of silicone oil (A), monomer (B) and aqueous phase (C). Formation of multiple core particle.

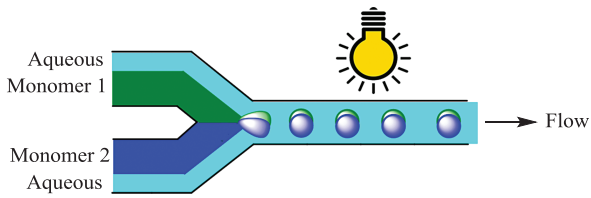

Figure 8.38 Flow pattern of Janus particle synthesis and droplet interface with different ratios for the volume fraction.

location) to generate polymer capsules with different shapes (*i.e.* spheres, truncated spheres and hemispheres). The polymerisation was performed using tripropylene glycol (TPGDA) or ethylene glycol dimethacrylate (EGDMA) as the monomer and 1-hydroxycyclohexyl phenyl ketone (HCPK) as initiator. An increase in control over the morphology (size, 20–200 μm) was gained by variation of the flow rates of the different components (liquid A to C) (Figure 8.37).

Kumacheva *et al.* published another paper in 2006 describing the synthesis of Janus particles and three phase particles in flow.[117,118] The Janus particles were produced in a microfluidic device through the union of two liquid monomers in the presence of a photo-initiator (Figure 8.38). To form the particles, an aqueous solution of sodium dodecylsulfate was injected to break up the organic flow. The formed particles were then irradiated to induce the polymerisation. The shape of the Janus particles could be influenced as well as the ratio of the volume fractions of the Janus droplets allowing the properties of the particles to be easily tuned.

These examples show that good control over the synthesis of particles is possible in flow enabling the preparation of particles with the same size and shape. Following on from the publication of Kumacheva *et al.*, several patents disclosed the formation of droplets using multiple parallel flow-focusing devices.[119–121] A variety of reactor geometries could be used, resulting in droplets with a range of dimensions, shape, morphology and composition.

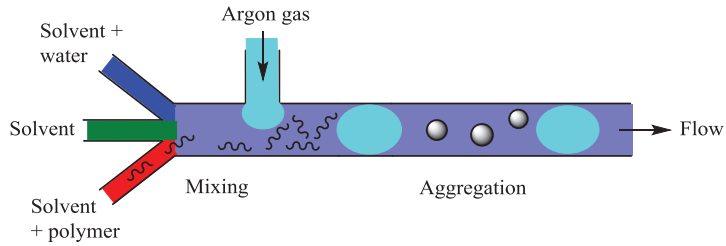

Figure 8.39 Microreactor for self-assembly nanoparticle preparation.

An inverse water in oil emulsion droplet formation in a microreactor has allowed the synthesis of monodispersed small (100 μm–1 mm) particles.[122] The droplets were first generated in the microfluidic device and dispensed into a petri dish which was subsequently irradiated by a 365 nm LED lamp to promote the photopolymerisation. Several further examples exist of equivalent particles being synthesised *via* such two stage processes. The first step being the required emulsification of the monomer or a liquid polymer in a microfluidic device to obtain droplets ideally with a narrow size distribution and then the second step, conducted in batch produces the hardening of the particle shells.[123–127]

The Moffitt group have used flow approaches to aid in the generation of block co-polymer for the construction of both vesicles and self-assembled nanoparticles for a variety of materials and biomedical uses.[128–131] An argon entrained gas–liquid flow is produced in which the compartmentalized liquid plugs are segmented by a regular stream of gas bubbles. This assists in the formation of spherical colloidal aggregates from the polymers (Figure 8.39). As an example the reactor unit used comprised of two stages; first, a sinusoidal 100 mm length mixing channel (100 μm wide×150 μm depth) which was followed by a residence time processing channel of 740 mm length (200 μm wide×150 μm depth). The fluid flows were delivered by programmable syringe pumps allowing easy modification of the flow rates and relative stoichiometries. Interestingly, many different particle geometries and structures could be obtained that were not possible under batch processing conditions.

Emulsion polymerisation for polystyrene nanoparticle synthesis under flow conditions has been used as a process intensification strategy by Liu *et al.*[132] Building on the work of Ouzined *et al.*[133] which had indicated that unstable emulsion formation in a flow reactor may be due to the emergence of large unstable monomer droplets in the early stages of the processing several different emulsifiers were investigated. Ultimately a mixed non-ionic (Triton X-100) and anionic (sodium dodecyl benzenesulfonate (SDBS)) was selected.

The reactor configuration was relatively simple. A batch feed tank (vigorously stirred) containing the reactants (styrene and divinyl benzene 10 : 1) and emulsifier (SDBS plus Triton X-100) as an emulsion in water was used to

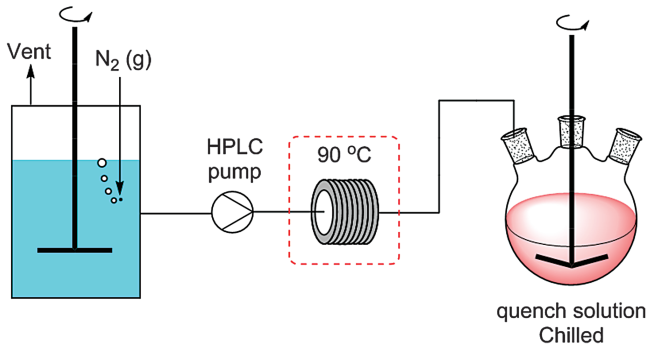

Figure 8.40 Microreactor for emulsion polymerisation of styrene and divinyl benzene.

source the thermally regulated tubular reactor (Figure 8.40). The output was collected into a chilled quench of aqueous hydroquinone. Monodispersed polystyrene nanoparticles (PDI 0.09–0.10) were successfully prepared in residence time of 5–20 min (68%–80% conversion) at 90 °C.

The generation of bead format polymers for applications in biomedical testing is gaining much interest especially as flow chemistry is now allowing the consistent and monodispersed formation of particles in sizes from nanometre to millimetre dimensions. Guo *et al.* have prepared porous polyacrylamide microspheres by polymerisation in a paraffin inverse suspension using microchannel technology to form core/shell droplets.[134] Inverse suspension polymerisation has also been evaluated by Hu *et al.* to create particles as templates for use in combinatorial chemistry and chemical biology.[135] Bead size (~500 μm with 20 μm range) was controlled through precise shear forces generated by flow rate changes of fluids entering a micromixer (Figure 8.41). The system could be run continuously with fresh injections of the monomers into the circulating system as required.

Wolff *et al.*[136] have investigated the preparation of thermo-responsive microgel particles through a continuous flow precipitation process to overcome difficulties associated with the batch scale-up (mixing, thermal regulation, concentration gradients *etc.*). A simple microtubular reactor (stainless steel coil; 1 mm ID, 5 or 10 m length) was selected for investigation (Figure 8.42) and a series of polymerisations performed and compared to batch processing under the same conditions. Key to the success of the flow process was the introduction of a static in-line micromixer used to blend the monomer/crosslinker and initiator making a homogeneous solution prior to it entering the heated reactor coil. In flow the microgel particle size could be tuned (70–370 nm) by modifying the residence time in the reactor, with shorter times leading to smaller radius. Indeed, sizes below 100 nm were hard to form using classical batch conditions without the use of large amount of surfactant demonstrating a true processing benefit of flow.

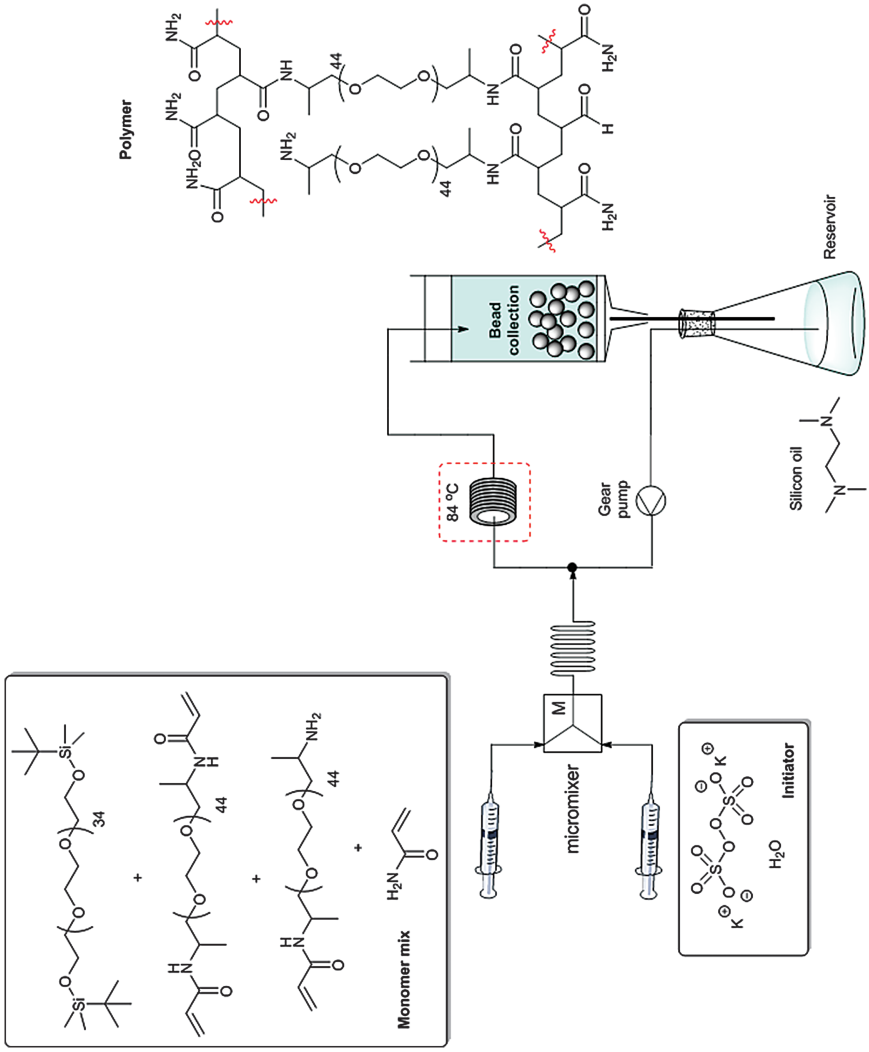

Figure 8.41 Continuous flow resin synthesiser.

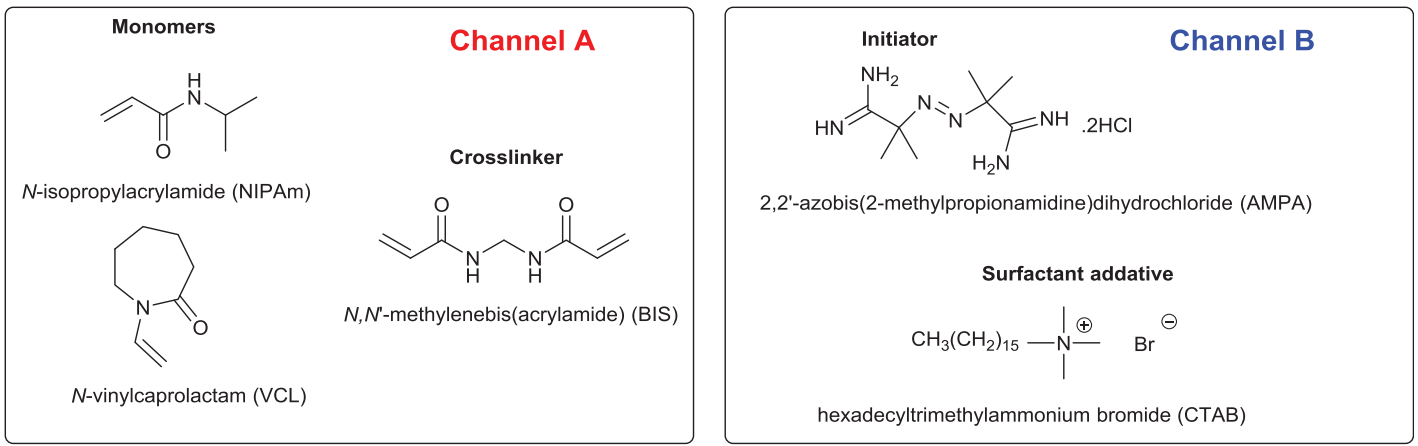

Figure 8.42 Continuous flow precipitation of microgel particles.

Köhler *et al.* used a co-flow system in which the droplets comprised of monomer [tri(propyleneglycol) diacrylate], initiator (aromatic ketone) and fluorescent dye were polymerised under photoactivation (366 nm, Lightningcure LC8, Hamamatsu) resulting in the formation of highly porous poly tri(propylene glycol) diacrylate particles if diethylene glycol was added.[137] The well-defined hydrodynamic conditions maintained in the reactor generated droplets with a narrow particle distribution. The same process was also run under thermal activation by mixing the monomer with a silver salt ($AgNO_3$) and adding a strong reducing agent (ascorbic acid). Thermally initiated polymerisation occurred at room temperature after 15 min. This could be a disadvantage as polymerisation of the mixture before the droplets are formed could lead to reactor blockage. However, changing the mixing order suppressed premature polymerisation and accumulation of silver nano-particles. It was not commented upon whether cooling the system prevented polymerisation. The set-up was used to quickly screen conditions for particle polymerisations and indicated that other polymer matrices beyond tri(propylene glycol) diacrylate could also be formed.

The synthesis of poly tri(propylene glycol) diacrylate particles has also performed by Visaveliya *et al.* in order to produce size-tuned fluorescent micro particles of broad size-spectrum.[138] Particle sizes between 40 and 500 μm were achieved by using various surfactants and changing the concentration along with flow rate ratios of the two immiscible phases. The possibility of mixing monochromatic fluorescent particles and multi-coloured particles of different sizes created a wide range of combinations for multi-fluorescence labelling. Therefore, the designed system has a wide applicability as a suitable combination could be found for specific applications.

Flow synthesis has thus opened up the possibility to achieve fast and scalable syntheses of polymer spherical capsules and beads. It is only a matter of time before more examples start to be reported.

8.7 Polymers for Light-emitting Diodes and Photovoltaic Devices

Semiconducting polymers are another type of macromolecule receiving increasing interest due to their use in lighting, solar cells and visual displays.[139–141] For these applications the polymers must be reproducibly prepared and their synthesis needs to be readily scalable. In addition, molecular weight distributions, defects in the conjugated backbone, control over end groups and impurity levels need to be strictly controlled.[142,143]

A method for the controlled synthesis of semiconducting polymers at large scale using a droplet based flow reactor was reported by de Mello *et al.*[143] The polymer studied was the commonly used poly(3-hexylthiophene) and was synthesised *via* Kumada cross-coupling (Figure 8.43). Flow processing

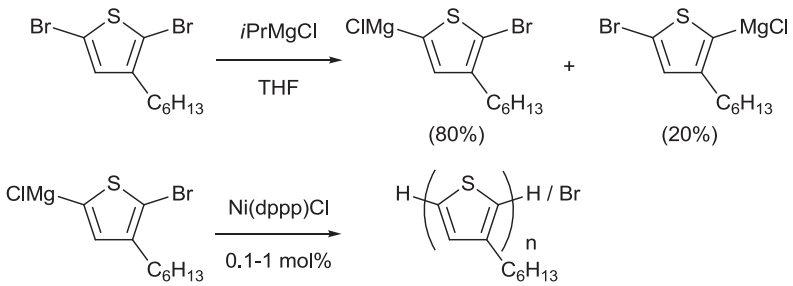

Figure 8.43 Synthesis of poly(3-hexylthiophene).

resulted in exceptional control over the polymer properties, comparable with the best commercially available material.

The authors found the synthesised polymers were consistent with a quasi-living polymerisation model.[144] In this model each catalyst molecule is predominantly, but not exclusively, linked with a single polymer chain.[145] Therefore, a better understanding of the polymer growth/kinetics was obtained. This resulted in polymers with a variety of M_n and M_w which flattened out at $M_n = 27\ kg\,mol^{-1}$ and $M_w = 46\ kg\,mol^{-1}$. The technique of using droplets resulted in an effective way of controlling molecular weight distributions. The process was also extended by including in-line preparation of the Grignard precursor. A continuous flow reactor with a four way mixer was inserted for the Grignard reaction in front of the droplet flow reactor. The continuous flow reactor (2 m long PTFE tube) was supplied with 2 M *i*PrMgCl ($5.33\ \mu L\,min^{-1}$), THF ($28.33\ \mu L\,min^{-1}$) and 2,5-dibromo-3-hexylthiophene ($2.35\ \mu L\,min^{-1}$) and heated to 55 °C. The intermediate was mixed with the catalyst, 1,3-*bis*[diphenyl-phosphinopropane]nickel(II) chloride ($Ni(dppp)Cl_2$), in a perfluorinated polyether co-solvent ($180\ \mu L\,min^{-1}$) and droplets were formed by a fluidic droplet generator. The droplets were processed further in the droplet flow reactor (a 1.1 m long PTFE tube) which was maintained at 55 °C for curing. This set-up enabled high production rates whilst maintaining low dispersities and high regioselectivities.

Essentially simultaneously Seyler *et al.*[146] were pursuing the same Ni Kumada catalyst transfer polycondensation chemistry (Figure 8.44). By adjusting the monomer to catalyst ratio the molecular weight could be controlled which was easily adjusted by modification of the relative flow rates. A polymer of M_n $31\ kg\,mol^{-1}$ and dispersity of 1.5 was produced which was determined to be 95% regioregular (by ^1H NMR) which was comparable to material previously prepared in batch.

More recently, de Mello revisited their initial work exploring the synthesis of poly(3-hexylthiophene) with a greener bio-derived solvent, namely, 2-methyltetrahydrofuran (2-MeTHF).[147] A different precatalyst $Ni(dppp)Br_2$, which was more soluble and therefore can be used at higher concentration, was also employed. A jacketed tube reactor (coaxial tube) was used to heat (65 °C) the reacting solution avoiding the need to use oil batch heating.

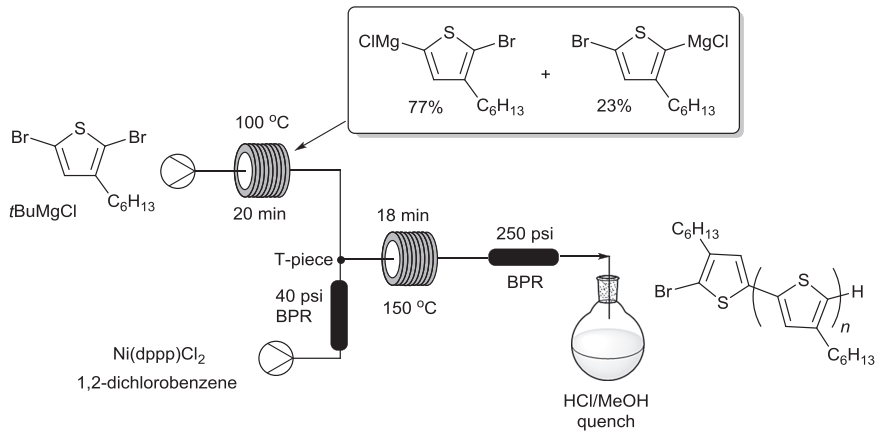

Figure 8.44 Flow synthesis of poly(3-hexylthiophene).

Polymers of 44–46 kg mol^{-1} (PDI of 1.4, 93% regioregular) were produced avoiding the use of previously used chlorinated solvents.

The synthesis of highly conjugated polymer as used in the area of organic photovoltaic has become a popular research topic, gaining control over the synthesis is very important to regulate the light emitting properties. Consequently flow chemistry has been applied to their synthesis. Typically using a Suzuki polycondensation technique a dihalogenated (normally dibromo) substrate undergoes transition metal catalysed coupling with a suitably functionalised bis-boronic acid. Seyler *et al.*[148] showed that the blue-emitting polymer poly(9,9-dioctylfluoene) (PFO) and two additional performance polymers (PCDTBT, PCDHTBT) could be prepared in a continuous flow operation using a commercially available bench top flow reactor (Figure 8.45). In one example run the synthesis of PFO ($M_n = 23$ kg mol^{-1}, $Đ = 2.8$) was achieved in 90% in 1 h residence time at 120 °C. Altering the reactor temperature and residence time was demonstrated to impact both M_n and M_w as well as the final isolated yield.

Grenier *et al.*[149] have also used flow chemistry to assist in the scale-up of heteroaryl polymer synthesis. The desired polymer was generated from 3,4-ethylenedioxythiophene (EDOT) as a strongly electron rich donor monomer and isoindigo (ISOI) as the corresponding electron accepting component (Figure 8.46). The material, along with the catalysts, were loaded into a sample loop and injected into a column packed (1 cm ID × 5 cm length) with a solid crushed melt of Cs_2CO_3/PivOH (2.3 : 0.3) and diatomaceous earth. Even at low flow rates (0.06 mL min^{-1}) the resulting short residence times gave only low M_n 21 kg mol^{-1}. However, the addition of a second column connected in series allowed longer reactions with polymers of M_n of 33 kg mol^{-1} to be obtained. Several experiments increasing the scale were performed giving consistent results, in fact at larger scales the yield was notably increased, which was ascribed to less diffusion of the regents in the reactors.

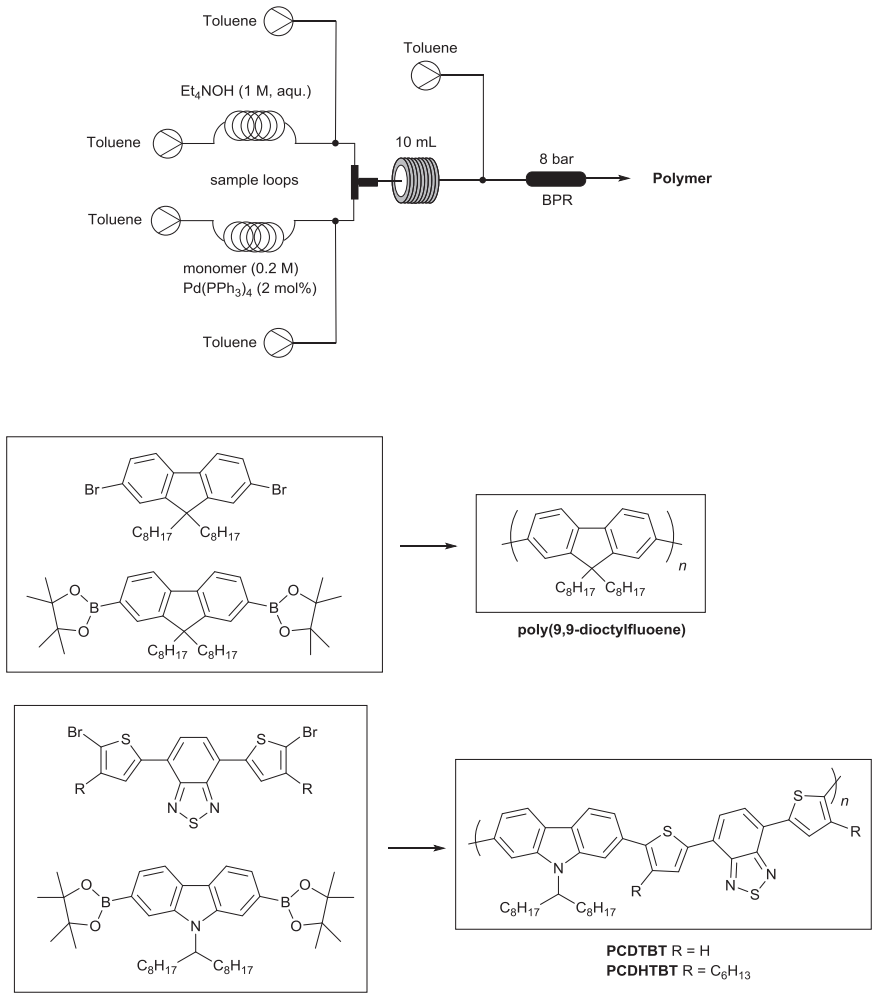

Figure 8.45 Polycondensation set-up for the preparation of conjugated polymers *via* Suzuki flow processing.

Using a similar approach, Gobalasingham *et al.*[150] also explored direct arylation polymerisation chemistry in flow for the synthesis of poly[(2,5-bis(2-hexyldecyloxy)phenylene)-*alt*-(4,7-di(thiophen-2-yl) benzo[c][1,2,5]thiadiazole)] (PPDTBT). The addition of neodecanoic acid was used to help improve the quality of the polymer product by reducing β-defects. In a standard run the reactants and catalyst were dissolved in toluene and pumped through the packed bed column. Initially, a glass column was used but later this was substituted with a stainless steel (12 mL internal volume) unit due to safety issue resulting from pressure build in the reactor (Figure 8.47). Typical yields of the polymer product in the range of 40–60% could be attained following Soxhlet extraction/purification. A polymer product with

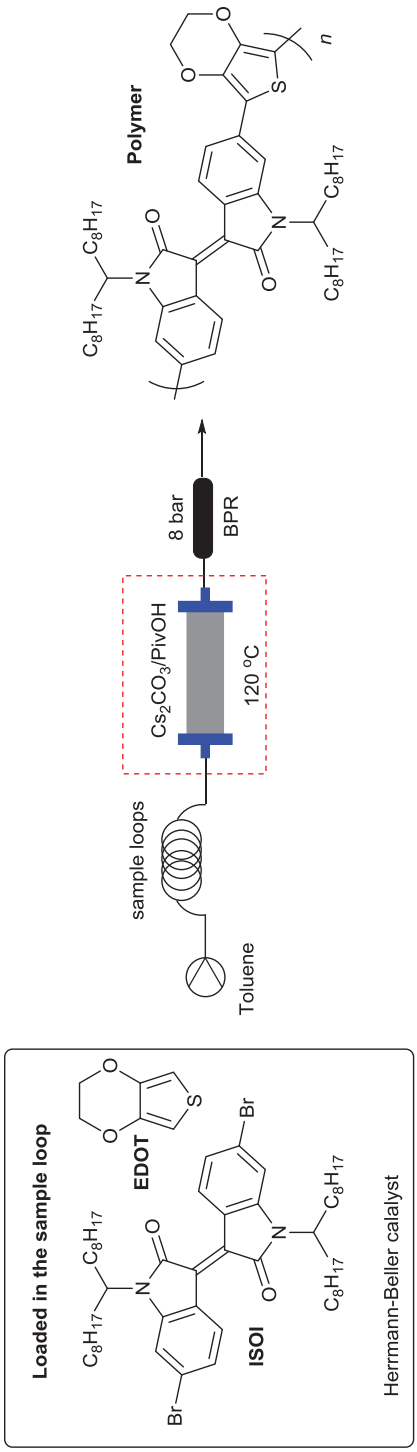

Figure 8.46 (Hetro)arylation polymerisation in flow.

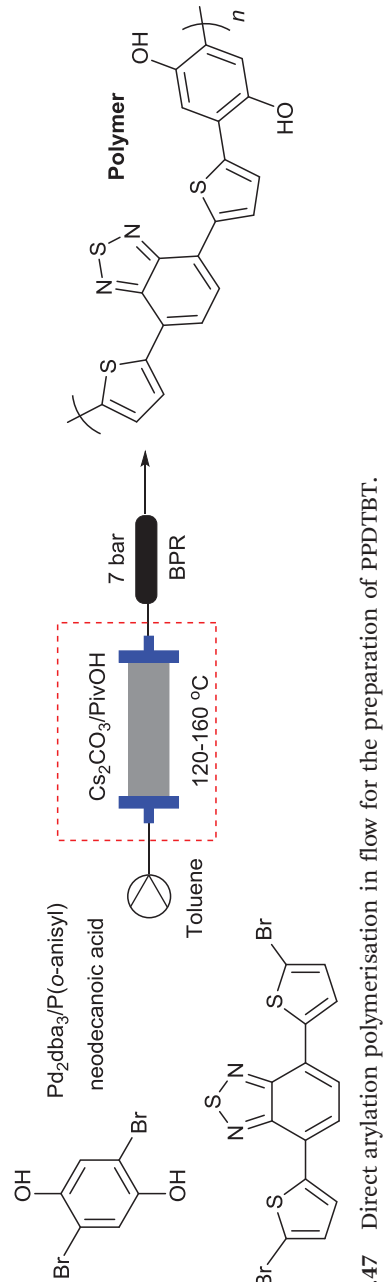

Figure 8.47 Direct arylation polymerisation in flow for the preparation of PPDTBT.

$M_n = 28$ kDa with a 120 min residence time at 120 °C was achieved for a monomer concentration of 150×10^{-3} M. As expected increasing the monomer concentration to 170×10^{-3} M whist maintaining the processing conditions increased the M_n to 60 kDa but was associated with a wider PDI ($2.3 \rightarrow 2.9$).

Controlling M_n and obtaining a defect free, uniform macromolecular structure can significantly impact on characteristics of a conjugated polymer effecting important aspects such as the polymer's band gap, which for photovoltaics, is a crucial parameter. Consequently gaining greater reproducibility and exacting control over the synthesis of the polymer is of paramount importance. Pirotte *et al.* showed it was possible to tune the band gap in a bulk heterojunction polymer system (PffBT4T–2OD, Figure 8.48) through its synthesis in flow using a Stille polymerisation process.[151] A flow synthesis approach was selected as it had been previously indicated that the batch scale-up was problematic.[152] A M_n value of >60 kDa was targeted in flow due to the limits of solubility of the potential high molecular weight products. Changing residence time (1–72 h) generally led to higher M_n (36–84.2 kDa), interestingly, increasing temperature (120–140 °C) gave a reduction in M_n which was associated with an increase of diffusion (lower reagent concentration). This was confirmed through experiments changing concentration of the monomer partners and also the injection volume of the reacting components. The system was capable of delivering around 1.2 $g\,h^{-1}$ productivity.

The conductive properties of poly(*p*-phenylene vinylene) (PPV) and its derivatives have made it an important molecular class to the modern electronic area especially with recent interest in further applications in biosenors, bioimaging and biomedical implants. Zaquen *et al.*[153] studied the two-step preparation of the analogue MDMO-PVP *via* radical sulfinyl polymerisation followed by elimination in flow (Figure 8.49). A reasonable yield of 42% for a polymer with an indicative M_n of 9.7 $kg\,mol^{-1}$ was obtained. The process still has significant room for improvement as the required flow rate in the second reactor prevented a lower flow rate being used in the first stage reactor meaning only a 45% monomer conversion was reached. This is obviously a non-ideal situation but could be easily overcome by using a larger initial reactor chip which was not available to the researchers at the time.

It is evident that with the ever increasing interest in the area of organic photovoltaics this will be an area which sees many more example of innovative chemistry being developed in flow to aid in the synthesis and scaling of these valuable polymers.

8.8 Summary and Future Perspectives

The many highlighted examples shown in this review chapter demonstrate the growing repertoire of syntheses that can be performed in flow delivering a range of advanced materials from soluble sequenced polymers to colloids and nanoparticulates in high yield and purity. What is becoming apparent is that the increasing adoption of automation technologies to enhance the

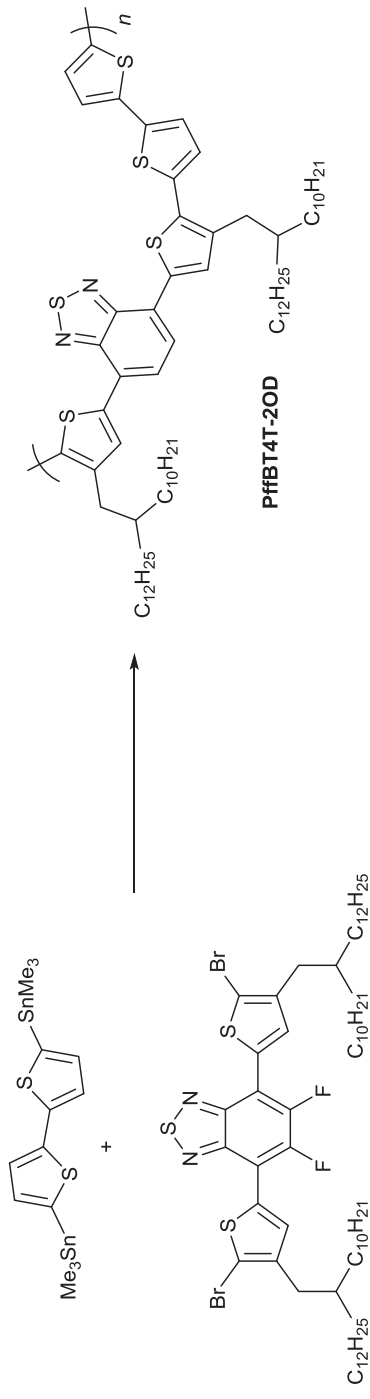

Figure 8.48 Structure of polymer PffBT4T–2OD.

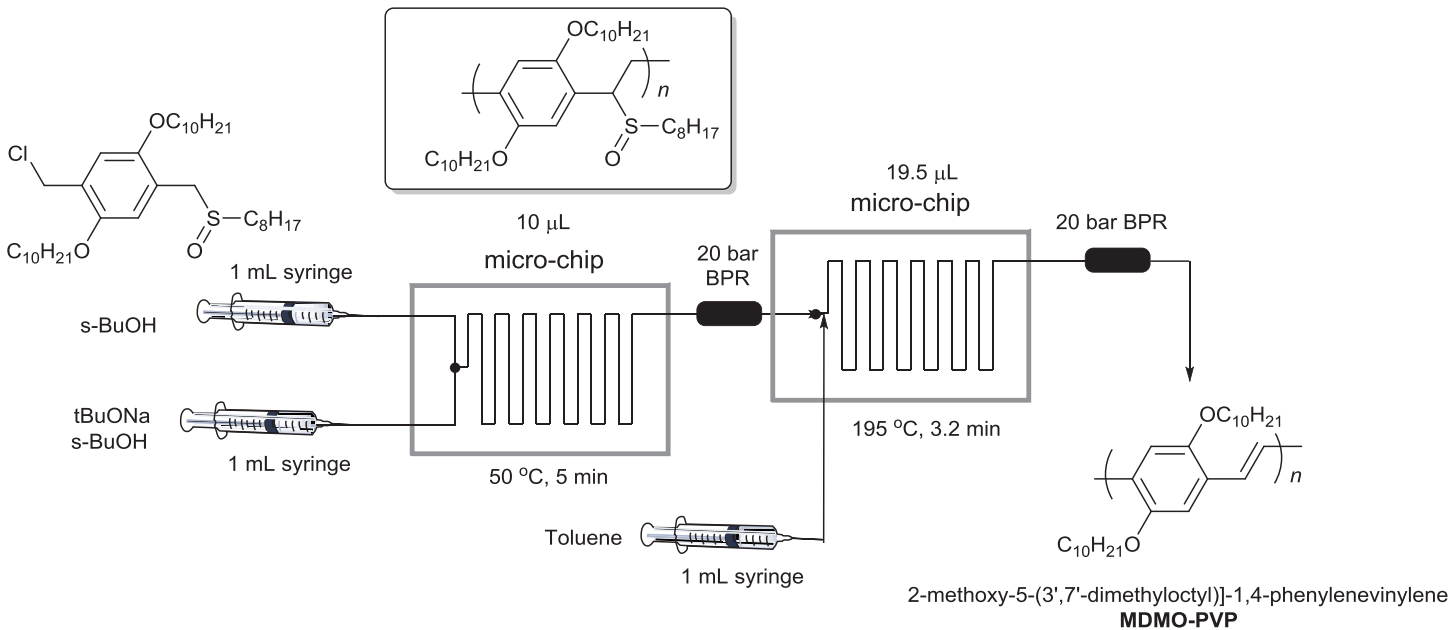

Figure 8.49 MDMO-PVP synthesis in flow.

speed and efficiency of synthesis is having a significant impact on polymer science. Indeed, such synthesis machines, when coupled with the full range of process analytical technologies (PAT), will soon be able to design, generate and optimise a polymer and its tailored physical property in a streamlined and fully independent work flow. This will obviously also have a knock-on effect into other related areas such as the synthesis of more elaborated droplet and nanoparticulate materials. Another aspect which is seeing rapid growth is the preparation of bio-derived polymers. Obviously from an environmental and societal stance greater demand will be increasingly placed on finding replacements for existing petrochemical derived polymers. Interestingly, not only will some of the new approaches such as enzyme catalysed polymerisation benefit but also their use in the recycling and controlled degradation will also be a more important area of research. It is expected that this area of polymer reclamation will be one of the dominant expansion areas in materials science over the next decade.

It is evident from the already extensive use of flow processing in polymer synthesis that it offers many advantages; in addition it fits well with many of the new and developing technologies which will further aid the next generation of polymer chemists. We strongly believe that flow polymerisation techniques will continue to evolve and have the potential to become the main synthesis approach in the near future surpassing traditional batch methods. Currently it is an exciting time to embrace these new tools and to exploit their benefits to find solutions to our modern polymer preparation challenges.

References

1. M. Szwarc, *Nature*, 1956, **178**, 1168–1169.
2. C. Geacintov, J. Smid and M. Szwarc, *J. Am. Chem. Soc.*, 1962, **84**, 2508–2514.
3. D. N. Bhattacharyya, C. L. Lee, J. Smid and M. Szwarc, *J. Phys. Chem.*, 1965, **69**, 612–623.
4. V. H. Hostalka, R. V. Figini and G. V. Schulz, *Die Makromol. Chem.*, 1964, **71**, 198–203.
5. G. V. Löhr and G. V. Schulz, *Die Makromol. Chem.*, 1964, **77**, 240–243.
6. G. Löhr, B. J. Schmitt and G. V. Schulz, *Z. Phys. Chem.*, 1972, **78**, 177–198.
7. A. Natalello, J. Morsbach, A. Friedel, A. Alkan, C. Tonhauser, A. H. E. Müller and H. Frey, *Org. Process Res. Dev.*, 2014, **18**, 1408–1412.
8. Carbocationic Polymerization: A Rejuvenation, in *Cationic Polymerization*, ed. R. Faust and T. D. Shaffer, *ACS Symposium Series*, American Chemical Society, Washington, DC, 1997, ch. 1, pp. 1–11.
9. A. Nagaki, K. Kawamura, S. Suga, T. Ando, M. Sawamoto and J.-I. Yoshida, *J. Am. Chem. Soc.*, 2004, **126**, 14702–14703.
10. Y. Tani, M. Takumi, S. Moronaga, A. Nagaki and J.-I. Yoshida, *Eur. Polym. J.*, 2016, **80**, 227–233.

11. S. Zhu, Y. Lu, K. Wang and G. Luo, *Eur. Polym. J.*, 2016, **80**, 219–226.
12. S. Zhu, Y. C. Lu, K. Wang and G. S. Luo, *RSC Adv.*, 2016, **6**, 9827–9834.
13. N. V. Ulitin and K. A. Tereshchenko, *Russ. J. Appl. Chem.*, 2015, **88**, 808–819.
14. A. Nagaki, A. Miyazaki and J.-I. Yoshida, *Macromolecules*, 2010, **43**, 8424–8429.
15. J. L. Nyrop, A. Soheili, R. Xiang, F. Meng, J. H. Waldman, X. Jia, R. G. Parmar, B. W. Thuronyi, J. M. Williams, L. Dimichele, M. Journet, B. J. Howell, B. Mao, I. W. Davies, S. L. Colletti, L. Sepp-Lorenzino and E. N. Guidry, *J. Polym. Sci., Part A: Polym. Chem.*, 2014, **52**, 1119–1129.
16. X. Hu, N. Zhu, Z. Fang and K. Guo, *React. Chem. Eng.*, 2017, **2**, 20–26.
17. D. Wilms, J. Nieberle, J. Klos, H. Löwe and H. Frey, *Chem. Eng. Technol.*, 2007, **30**, 1519–1524.
18. K. Aoi and M. Okada, *Prog. Polym. Sci.*, 1996, **21**, 151–208.
19. T. Kagiya, S. Narisawa, T. Maeda and K. Fukui, *J. Polym. Sci., Part B: Polym. Lett.*, 1966, **4**, 441–445.
20. F. Wiesbrock, R. Hoogenboom, M. A. M. Leenen, M. A. R. Meier and U. S. Schubert, *Macromolecules*, 2005, **38**, 5025–5034.
21. F. Wiesbrock, R. Hoogenboom, C. H. Abeln and U. S. Schubert, *Macromol. Rapid Commun.*, 2004, **25**, 1895–1899.
22. F. Wiesbrock, R. Hoogenboom, M. Leenen, S. F. G. M. van Nispen, M. van der Loop, C. H. Abeln, A. M. J. van den Berg and U. S. Schubert, *Macromolecules*, 2005, **38**, 7957–7966.
23. R. M. Paulus, T. Erdmenger, C. R. Becer, R. Hoogenboom and U. S. Schubert, *Macromol. Rapid Commun.*, 2007, **28**, 484–491.
24. R. Hoogenboom, M. W. Fijten, R. M. Paulus, H. M. Thijs, S. Hoeppener, G. Kickelbick and U. S. Schubert, *Polymer*, 2006, **47**, 75–84.
25. E. Baeten, B. Verbraeken, R. Hoogenboom and T. Junkers, *Chem. Commun.*, 2015, **51**, 11701–11704.
26. A.-C. Albertsson and I. K. Varma, *Biomacromolecules*, 2003, **4**, 1466–1486.
27. O. Nuyken and S. D. Pask, *Polymers*, 2013, **5**, 361–403.
28. R. Jianming, X. Anguo, W. Hongwei and Y. Hailin, *Des. Monomers Polym.*, 2014, **17**, 345–355.
29. G. L. Gregory, E. M. López-Vidal and A. Buchard, *Chem. Commun.*, 2017, **53**, 2198–2217.
30. S. A. Madbouly, K. Liu, Y. Xia and M. R. Kessler, *RSC Adv.*, 2014, **4**, 6710–6718.
31. H. Peng, J. Ling, J. Liu, N. Zhu, X. Ni and Z. Shen, *Polym. Degrad. Stab.*, 2010, **95**, 643–650.
32. C. Vilela, A. F. Sousa, A. C. Fonseca, A. C. Serra, J. F. J. Coelho, C. S. R. Freire and A. J. D. Silvestre, *Polym. Chem.*, 2014, **5**, 3119–3141.
33. N. Zhu, Z. Zhang, W. Feng, Y. Zeng, Z. Li, Z. Fang, K. Zhang, Z. Li and K. Guo, *RSC Adv.*, 2015, **5**, 31554–31557.

34. N. Zhu, Y. Liu, W. Feng, W. Huang, Z. Zhang, X. Hu, Z. Fang, Z. Li and K. Guo, *Eur. Polym. J.*, 2016, **80**, 234–239.
35. N. Zhu, W. Feng, X. Hu, Z. Zhang, Z. Fang, K. Zhang, Z. Li and K. Guo, *Polymer*, 2016, **84**, 391–397.
36. S. A. Van den Berg, H. Zuilhof and T. Wennekes, *Macromolecules*, 2016, **49**, 2054–2062.
37. P. Liu, G. Yang and H. Shao, *Eur. Polym. J.*, 2017, **93**, 815–821.
38. E. Baeten, S. Vanslambrouck, C. Jérôme, P. Lecomte and T. Junkers, *Eur. Polym. J.*, 2016, **80**, 208–218.
39. L. D. Arvanitopoulos, M. P. Greuel, B. M. King, A. K. Shim and H. J. Harwood, *Controlled Radical Polymerization. ACS Symposium Series*, 1998, vol. 685, pp. 316–331.
40. E. M. Schuster and P. Wipf, *Isr. J. Chem.*, 2014, **54**, 361–370.
41. J. P. Knowles, L. D. Elliott and K. I. Booker-Milburn, *Beilstein J. Org. Chem.*, 2012, **8**, 2025–2052.
42. O. Eckardt, B. Wenn, P. Biehl, T. Junkers and F. H. Schacher, *React. Chem. Eng.*, 2017, **2**, 479–486.
43. N. O'Brien, A. McKee, D. C. Sherrington, A. T. Slark and A. Titterton, *Polymer*, 2000, **41**, 6027–6031.
44. A. Chemto, A. Rannée, L. Chalan, D. Fischer and S. Bistac, *Eur. Polym. J.*, 2016, **80**, 247–255.
45. C. M. R. Abreu, A. C. Serra, A. V. Popov, K. Matyjaszewski, T. Guliashvili and J. F. J. Coelho, *Polym. Chem.*, 2013, **4**, 5629–5636.
46. Y.-M. Chuang, B. Wenn, S. Gielen, A. Ethirajan and T. Junkers, *Polym. Chem.*, 2015, **6**, 6488–6497.
47. T. Junkers and B. Wenn, *React. Chem. Eng.*, 2016, **1**, 60–64.
48. B. Wenn, M. Conradi, A. D. Carreiras, D. M. Haddleton and T. Junkers, *Polym. Chem.*, 2014, **5**, 3053–3060.
49. A. Anastasaki, V. Nikolaou, Q. Zhang, J. Burns, S. R. Samanta, C. Waldron, A. J. Haddleton, R. McHale, D. Fox, V. Percec, P. Wilson and D. M. Haddleton, *J. Am. Chem. Soc.*, 2014, **136**, 1141–1149.
50. G. Ramakers, A. Krivcov, V. Trouillet, A. Welle, H. Möbius and T. Junkers, *Macromol. Rapid Commun.*, 2017, **38**, 1700423-1–1700423-6.
51. N. Corrigan, S. Shanmugam, J. Xu and C. Boyer, *Chem. Soc. Rev.*, 2016, **45**, 6165–6212.
52. N. Corrigan, A. Almasri, W. Taillades, J. Xu and C. Boyer, *Macromolecules*, 2017, **50**, 8438–8448.
53. N. Corrigan, D. Rosli, J. W. J. Jones, J. Xu and C. Boyer, *Macromolecules*, 2016, **49**, 6779–6789.
54. N. Corrigan, R. Manahan, Z. T. Lew, J. Yeow, J. Xu and C. Boyer, *Macromolecules*, 2018, **51**, 4553–4563.
55. Y. Chu, N. Corrigan, C. Wu, C. Boyer and J. Xu, *ACS Sustainable Chem. Eng.*, 2018, **6**, 15245–15253.
56. S. Kundu, A. S. Bhangale, W. E. Wallace, K. M. Flynn, C. M. Guttman, R. A. Gross and K. L. Beers, *J. Am. Chem. Soc.*, 2011, **133**, 6006–6011.

57. A. S. Bhangle, K. L. Beers and R. A. Gross, *Macromolecules*, 2012, **45**, 7000–7008.
58. M. J. Zhang, E. Z. Su, J. P. Lin and D. Z. Wei, *Chem. Biochem. Eng. Q.*, 2012, **26**, 1–6.
59. J. H. Wosnick and S. Faucher, *U. S. Pat. Appl.*, 12/240,421, 29 Sep 2008.
60. N. Zhu, W. Huang, X. Hu, Y. Liu, Z. Fang and K. Guo, *Macromol. Rapid Commun.*, 2018, **39**, 1700807-1–1700807-6.
61. M. Yamada, M. Nakashima and M. Seki, *Anal. Chem.*, 2004, **76**, 5465–5471.
62. D. C. Hassell and E. M. Bow, *Appl. Spectrosc.*, 1998, **52**, 18A–29A.
63. R. Hoogenboom, M. W. M. Fijten, C. H. Abeln and U. S. Schubert, *Macromol. Rapid Commun.*, 2004, **25**, 237–242.
64. M. A. R. Meier, R. Hoogenboom, M. W. M. Fijten, M. Schneider and U. S. Schubert, *J. Comb. Chem.*, 2003, **5**, 369–374.
65. H. Zhang, M. W. M. Fijten, R. Hoogenboom, R. Reinierkes and U. S. Schubert, *Macromol. Rapid Commun.*, 2003, **24**, 81–86.
66. A. M. Alb, M. F. Drenski and W. F. Reed, *Polym. Int.*, 2008, **57**, 390–396.
67. M. J. Kamaruddin, J. El harfi, G. Dimitrakis, N. T. Nguyen, S. W. Kingman, E. Lester, J. P. Robinson and D. J. Irvine, *Green Chem.*, 2011, **13**, 1147–1151.
68. E. G. Chatzi, O. Kammona and C. Kiparissides, *J. Appl. Polym. Sci.*, 1997, **63**, 799–809.
69. A. Tuchbreiter, R. Mülhaupt, A. Warmbold, P. Liebertraut, B. Koppler and J. Honerkamp, *Polym. Prepr.*, 2002, **43**, 285–286.
70. H. Hua and M. A. Dubé, *J. Polym. Sci., Part A: Polym. Chem.*, 2001, **39**, 18601876.
71. R. F. Storey and T. L. Maggio, *Macromolecules*, 2000, **33**, 681–688.
72. J. Höpfner, K. F. Ratzsch, C. Botha and M. Wilhelm, *Macromol. Rapid Commun.*, 2018, **39**, 1700766, (1–7).
73. C. H. Hornung, K. von Känel, I. Martinez-Botella, M. Espiritu, X. Nguyen, A. Postma, S. Saubern, J. Chiefari and S. H. Thang, *Macromolecules*, 2014, **47**, 8203–8213.
74. F. Bally, C. A. Serra, C. Brochon, N. Anton, T. Vandamme and G. A. Hadziioannou, *Macromol. React. Eng.*, 2011, **5**, 542–547.
75. J. J. Haven, J. Vandenbergh and T. Junkers, *Chem. Commun.*, 2015, **51**, 4611–4614.
76. M. E. Levere, I. Willoughby, S. ODonohue, P. M. Wright, A. J. Grice, C. Fidge, C. Remzi Becer and D. M. Haddleton, *J. Polym. Sci., Part A: Polym. Chem.*, 2011, **49**, 1753–1763.
77. M. Rubens, J. H. Vrijsen, J. Laun and T. Junkers, *Angew. Chem., Int. Ed.*, 2019, **58**, 3183–3187.
78. K. Modjarrad and S. Ebnesajjad, *Handbook of Polymer Applications in Medicine and Medical Devices*, Elsevier, Amsterdam, 2013, pp. 1–353.
79. R. S. Ashraf, B. C. Schroeder, H. A. Bronstein, Z. Huang, S. Thomas, R. J. Kline, C. J. Brabec, P. Rannou, T. D. Anthopoulos, J. R. Durrant and I. McCulloch, *Adv. Mater.*, 2013, **25**, 2029–2034.

80. J. J. Chen, A. L. Ahmad and B. S. Ooi, *J. Membr. Sci.*, 2014, **469**, 73–79.
81. C. H. Hornung, X. Nguyen, S. Kyi, J. Chiefari and S. Saubern, *Aust. J. Chem.*, 2013, **66**, 192–198.
82. M. Stephan, S. Grosse, M. Stintz and U. Blankschein, *J. Appl. Polym. Sci.*, 2007, **103**, 258–262.
83. S. E. Barnes, Z. T. Cygan, J. K. Yates, K. L. Beers and E. J. Amis, *Analyst*, 2006, **131**, 1027–1033.
84. C. H. H. Neufeld and C. S. Marvel, *J. Polym. Sci., Part A-1: Polym. Chem.*, 1966, **4**, 2907–2908.
85. M. S. Nightingale, S.-C. Tsai and J. L. Gaylor, *J. Biol. Chem.*, 1967, **242**, 341–349.
86. M. Mulder in *Membranes in Bioprocessing: Theory and Applications*, ed. J. A. Howell, V. Sanchez and R. W. Field, Springer, Netherlands, 1993, pp. 13–54, DOI: 10.1007/978-94-011-2156-9_2.
87. R. K. Scopes, *Protein Purification: Principles and Practice*, Springer Science and Business Media, New York, 2013.
88. T. R. Cipriani, C. G. Mellinger, L. M. de Souza, C. H. Baggio, C. S. Freitas, M. C. A. Marques, P. A. J. Gorin, G. L. Sassaki and M. A. Lacomini, *J. Nat. Prod.*, 2006, **69**, 1018–1021.
89. Q. P. Peniston and J. L. McCarthy, *J. Am. Chem. Soc.*, 1948, **70**, 1324–1328.
90. R. Ghidoni, S. Sonnino and G. Tettamanti, *Lipids*, 1978, **13**, 820–822.
91. N. A. O. Pitombeira, J. G. V. Neto, D. A. Silva, J. P. A. Feitosa, H. C. B. Paula and R. C. M. de Paula, *Carbohydr. Polym.*, 2015, **117**, 610–615.
92. J. Bustamante, P. Navarro, G. Arana, A. de Diego and J. M. Madariaga, *Talanta*, 2013, **114**, 32–37.
93. M. L. Fishman and F. R. Eirich, *J. Phys. Chem.*, 1971, **75**, 3135–3140.
94. S. N. Millner, *Appl. Microbiol.*, 1969, **17**, 639–640.
95. B. Kwon, H. K. Shon and J. Cho, *Sep. Sci. Technol.*, 2009, **44**, 3224–3238.
96. S. Song, A. K. Singh, T. J. Shepodd and B. J. Kirby, *Anal. Chem.*, 2004, **76**, 2367–2373.
97. R. Brinkman and J. V. Steinfoorn, *Biochem. J.*, 1936, **30**, 1523–1525.
98. N. García-Otero, J. Alonso-Lorenzo, M. C. Barciela-Alonso, P. Bermejo-Barrera and A. Moreda-Piñeiro, *Microchem. J.*, 2015, **122**, 50–56.
99. C.-W. Cho, D.-Y. Lee and C.-W. Kim, *Carbohydr. Polym.*, 2003, **54**, 21–26.
100. L. Brocken, P. D. Price, J. Whittaker and I. R. Baxendale, *React. Chem. Eng.*, 2017, **2**, 656–661.
101. E. Kumacheva and P. Garstecki, *Microfluidic Reactors for Polymer Particles*, John Wiley and Sons, Ltd, New York, 2011, ch. 2, pp. 7–15, ch. 4–7, pp. 22–145, ISBN: 9780470057735.
102. J. M. Asua, *Macromol. React. Eng.*, 2016, **10**, 311–323.
103. A. Kumari, S. K. Yadav and S. C. Yadav, *Colloids Surf., B*, 2010, **75**, 1–18.
104. *Polymer Based Systems on Tissue Engineering, Replacement and Regeneration*, ed. R. L. Reis and D. Cohn, Springer publishing, Netherlands, 2002, ch. 1–22, pp. 1–426.

105. C. Silvestre, D. Duraccio and S. Cimmino, *Prog. Polym. Sci.*, 2011, **36**, 1766–1782.
106. S. Srivastava, J. L. Schaefer, Z. Yang, Z. Tu and L. A. Archer, *Adv. Mater.*, 2014, **26**, 201–234.
107. W. Meier, *Chem. Soc. Rev.*, 2000, **29**, 295–303.
108. H. N. Yow and A. F. Routh, *Soft Matter*, 2006, **2**, 940–949.
109. A. C. Balazs, T. Emrick and T. P. Russell, *Science*, 2006, **314**, 1107–1110.
110. A. Loxley and B. Vincent, *J. Colloid Interface Sci.*, 1998, **208**, 49–62.
111. P. J. Dowding, R. Atkin, B. Vincent and P. Bouillot, *Langmuir*, 2004, **20**, 11374–11379.
112. C. S. Peyratout and L. Dähne, *Angew. Chem., Int. Ed.*, 2004, **43**, 3762–3783.
113. L.-Y. Chu, R. Xie, J.-H. Zhu, W.-M. Chen, T. Yamaguchi and S.-I. Nakao, *J. Colloid Interface Sci.*, 2003, **265**, 187–196.
114. G. H. Ma, Z. G. Su, S. Omi, D. Sundberg and J. Stubbs, *J. Colloid Interface Sci.*, 2003, **266**, 282–294.
115. R. Liu, G. Ma, F.-T. Meng and Z.-G. Su, *J. Controlled Release*, 2005, **103**, 31–43.
116. M. Seo, Z. Nie, S. Xu, M. Mok, P. C. Lewis, R. Graham and E. Kumacheva, *Langmuir*, 2005, **21**, 11614–11622.
117. Z. Nie, S. Xu, M. Seo, P. C. Lewis and E. Kumacheva, *J. Am. Chem. Soc.*, 2005, **127**, 8058–8063.
118. Z. H. Nie, W. Li, M. Seo, S. Q. Xu and E. Kumacheva, *J. Am. Chem. Soc.*, 2006, **128**, 9408–9412.
119. P. Garstecki, D. Weibel, I. Gitlin, S. Takeuchi, S. Xu, Z. Nie, M. Seo, P. Lewis, E. Kumacheva, H. Stone and G. Whitesides, *U. S. Pat. App.* 11/368,263, 2007.
120. E. Kumacheva, *U. S. Pat.* 7,033,524, 2006.
121. E. Kumacheva, *U. S. Pat. App.* 12/451,886, 2010.
122. K. Takimoto, E. Takano, Y. Kitayama and T. Takeuchi, *Langmuir*, 2015, **31**, 4981–4987.
123. T. Nisisako, T. Torii, T. Takahashi and Y. Takizawa, *Adv. Mater.*, 2006, **18**, 1152–1156.
124. A. Kubo, H. Shinmori and T. Takeuchi, *Chem. Lett.*, 2006, **35**, 588–589.
125. T. Nisisako, T. Torii and T. Higuchi, *Lab Chip*, 2002, **2**, 24–26.
126. H. J. Liu, M. Nakajima and T. Kimura, *J. Am. Oil Chem. Soc.*, 2004, **81**, 705–711.
127. J. X. Yun, C. M. Tu, D. Q. Lin, L. H. Xu, Y. T. Guo, S. C. Shen, S. H. Zhang, K. J. Yao, Y. X. Guan and S. J. Yao, *J. Chromatogr. A*, 2012, **1247**, 81–88.
128. C.-W. Wang, D. Sinton and M. G. Moffitt, *J. Am. Chem. Soc.*, 2011, **133**, 18853–18864.
129. C.-W. Wang, A. Bains, D. Sinton and M. G. Moffitt, *Langmuir*, 2012, **28**, 15756–15761.
130. C.-W. Wang, D. Sinton and M. G. Moffitt, *ACS Nano*, 2013, **7**, 1424–1436.
131. Z. Xu, B. Yan, J. Riordon, Y. Zhao, D. Sinton and M. G. Moffitt, *Chem. Mater.*, 2015, **27**, 8094–8104.

132. X. Liu, Y. Lu and G. Luo, *Ind. Eng. Chem. Res.*, 2017, **56**, 9489–9495.
133. K. Ouzineb, C. Graillat and T. McKenna, *J. Appl. Polym. Sci.*, 2004, **91**, 2195–2207.
134. S. Guo, T. Yao, C. Wang, C. Zeng and L. Zhang, *React. Funct. Polym.*, 2015, **91–92**, 77–84.
135. H. Hu, S. Nikitin, A. B. Berthelsen, F. Diness, S. Schoffelen and M. Meldal, *ACS Comb. Sci.*, 2018, **20**, 492–498.
136. H. J. M. Wolff, M. Kather, H. Breisig, W. Richtering, A. Pich and M. Wessling, *ACS Appl. Mater. Interfaces*, 2018, **10**, 24799–24806.
137. J. M. Köhler, I. Kraus, J. Faerber and C. Serra, *J. Mater. Sci.*, 2012, **48**, 2158–2166.
138. N. Visaveliya and J. M. Köhler, *J. Mater. Chem. C*, 2015, **3**, 844–853.
139. D. Braun and A. J. Heeger, *Appl. Phys. Lett.*, 1991, **58**, 1982–1984.
140. Y. Liang and L. Yu, *Acc. Chem. Res.*, 2010, **43**, 1227–1236.
141. V. Chouvardas, A. Miliou and M. Hatalis, *Displays*, 2008, **29**, 185–194.
142. S. Xu, Z. Nie, M. Seo, P. Lewis, E. Kumacheva, H. A. Stone, P. Garstecki, D. B. Weibel, I. Gitlin and G. M. Whitesides, *Angew. Chem.*, 2005, **117**, 734–738.
143. J. H. Bannock, S. H. Krishnadasan, A. M. Nightingale, C. P. Yau, K. Khaw, D. Burkitt, J. J. M. Halls, M. Heeney and J. C. de Mello, *Adv. Funct. Mater.*, 2013, **23**, 2123–2129.
144. M. C. Iovu, E. E. Sheina, R. R. Gil and R. D. McCullough, *Macromolecules*, 2005, **38**, 8649–8656.
145. B. C. Achord and J. W. Rawlins, *Macromolecules*, 2009, **42**, 8634–8639.
146. H. Seyler, J. Subbiah, D. J. Jones, A. B. Holmes and W. W. H. Wong, *Beilstein J. Org. Chem.*, 2013, **9**, 1492–1500.
147. J. H. Bannock, W. Xu, T. Baïssas, M. Heeney and J. C. de Mello, *Eur. Polym. J.*, 2016, **80**, 240–246.
148. H. Seyler, D. J. Jones, A. B. Holmes and W. W. H. Wong, *Chem. Commun.*, 2012, **48**, 1598–1600.
149. F. Grenier, B. R. Aïch, Y.-Y. Lai, M. Guérette, A. B. Holmes, Y. Tao, W. W. H. Wong and M. Leclerc, *Chem. Mater.*, 2015, **27**, 2137–2143.
150. N. S. Gobalasingham, J. E. Carlé, F. C. Krebs, B. C. Thompson, E. Bundgaard and M. Helgesen, *Macromol. Rapid Commun.*, 2017, **38**, 1700526-1–1700526-7.
151. G. Pirotte, S. Agarkar, B. Xu, J. Zhang, L. Lutsen, D. Vanderzande, H. Yan, P. Pollet, J. R. Reynolds, W. Maes and S. R. Marder, *J. Mater. Chem. A*, 2017, **5**, 18166–18175.
152. M. Helgesen, J. E. Carlé, G. A. dos Reis Benatto, R. R. Søndergaard, M. Jørgensen, E. Bundgaard and F. C. Krebs, *Adv. Energy Mater.*, 2015, **5**, 1401996.
153. N. Zaquen, E. Baeten, J. Vandenbergh, L. Lutsen, D. Vanderzande and T. Junkers, *Chem. Eng. Technol.*, 2015, **38**, 1749–1757.